Fuller

DOE/ER/60655-5

REGIONAL AEROSOL DEPOSITION IN HUMAN UPPER AIRWAYS

Final Report
David L. Swift, Ph.D.,
Principal Investigator

Johns Hopkins University
School of Hygiene and Public Health
615 North Wolfe Street
Baltimore, M
Maryland 21205

November, 1997

Prepared for
THE U.S. DEPARTMENT OF ENERGY
GRANT No. DE-FG02-88ER60655

DISCLAIMER

FINAL REPORT

Project Title: Regional Aerosol Deposition in Human Upper Airways
Principal Investigator: David L. Swift, Ph.D., Professor
Awarded Institution: Johns Hopkins University
School of Hygiene and Public Health
615 North Wolfe Street
Baltimore, MD 21205
Project Award Number: DE-FG02-88ER60655

Abstract

During the award period, a number of studies have been carried out related to the overall objective of the project which is to elucidate important factors which influence the upper airway deposition and dose of particles in the size range 0.5 nm - 10 μm, such as particle size, breathing conditions, age, airway geometry, and mode of breathing. These studies are listed below.

(1) A high voltage electrospray system was constructed to generate polydispersed 1-10 μm diameter di-ethylhexyl sebacate aerosol for particle deposition studies in nasal casts and in human subjects.

(2) The effect of nostril dimensions, nasal passage geometry, and nasal resistance on particle deposition efficiency in forty healthy, nonsmoking adults at a constant flowrate were studied.

(3) The effect of nostril dimensions, nasal passage dimensions and nasal resistance on the percentage of particle deposition in the anterior 3 cm of the nasal passage of spontaneously breathing humans were studied.

(4) The region of deposition of monodispersed aerosols were studied using replicate casts.

(5) Ultrafine aerosol deposition using simulated breath holding path and natural path was compared.

(6) An experimental technique was proposed and tested to measure the oral deposition of inhaled ultrafine particles.

(7) We have calculated the total deposition fraction of ultrafine aerosols from 5 to 200 nm in the extrathoracic airways and in the lung.

(8) The deposition fraction of radon progeny in the head airways was studied using several head airway models.

FINAL REPORT

Research Objective

The objective of this research program was to elucidate important factors which influence overall and local deposition of aerosols in the human airways above the trachea. This includes the nasal passage, oral passage, pharynx, and larynx and is important information for the development of dosimetric models for radon progeny and other environmentally significant airborne particles. Of particular interest are the effects of flow rate, particle diameter, and airway dimension especially as affected by age and respiratory condition.

Design of a Particle Generating System for 1-10 μm Particles

A high voltage electrospray method was used to generate polydispersed 1-10 μm diameter di-ethylhexyl sebacate aerosol in a 51 X 51 X 51 cm^3 plexiglass box. Sixty-five percent (vol/vol) di-ethylhexyl sebacate in ethanol was fed by two needles kept at approximately 1.07 KV and 1.48 KV. The needles were positioned 90° to each other. A 9 KV negative electrode covered by a cylindrical shaped metal tube connected to ground was placed 7 cm in front of the 1.48 KV needles. Air at a flow rate of 30 L/min was passed around the negative electrode inside the grounded cylinder. A ground electrode was placed 7 cm in front of the 1.07 KV needle.

This measurement is carried out by a time-of-flight particle sizing instrument which measures aerodynamic equivalent diameters in the size range 0.8-15.0 μm (TSI Aerodynamic Particle Sizer, Model 3100). Comparison of the concentration of each size particle upstream and downstream of the passage gives the deposition efficiency as a function of aerodynamic particle diameter, and this function is a measure of the upper airway particle deposition efficiency at a given flow rate. An exposure system consisting of a wide bore tubing leading from the aerosol box, a tight fitting, low dead space nasal mask, and a mouthpiece leading to a constant flow pump system has been assembled and tested. Appropriate ports for isokinetic sampling of the inlet and outlet flows for the particle sizer have been integrated into the exposure system, and the system is prepared for experimental measurements. Illustrations of electrospray aerosol generating system and exposure system are shown in a manuscript submitted for publication. (Kesavanathan et al. The effect of nasal passage characteristics on particle deposition)

Nasal Entrance Geometry and the Deposition of 1-10 μm Aerosols

The effect of nasal geometry of both the internal and anterior structures upon particle deposition of 1 - 10 μm aerosols was studied in six human subjects. The deposition was first measured in the "normal" state, followed by measurements after decongestion (which produced an increase in the cross sectional area of the passage posterior to the nares). In all but one subject, the use of a decongesting agent, although it increased the airway cross sectional area, thus reducing the average air velocity, did not produce a measurable decrease in nasal deposition, as might be predicted by inertial theory. However, when the nasal entrance (nostril) of the

subjects was slightly enlarged and "circularized" with the use of a small metal ring, the deposition was observed to decrease significantly.

The effect of nostril dimensions, nasal passage geometry, and nasal resistance (R) on particle deposition efficiency (PDE) in forty healthy, nonsmoking adults (24 male, 16 females) at a constant flowrate were studied. An aerodynamic particle sizer measured the diameter and concentration of a polydispersed (1-10 μm diameter) aerosol drawn unidirectionally into the nose and out the mouth. For each particle size, the concentration of particles entering the nose (C_{in}) and leaving the mouth (C_{out}) was measured. Nasal PDE, defined as $(C_{in}-C_{out})/C_{in}*100$, was calculated for bilateral and unilateral flow.

A mixed, nonlinear model was used to fit the PDE to two models based on two sets of specifications. The geometric model included particle aerodynamic diameter (d_a), nostril dimensions, and minimum nasal cross-sectional area (A_{min}); the resistance model included d_a and R. The results showed that in both bilateral and unilateral geometric models, d_a, A_{min}, and E significantly affected PDE. In the resistance model, d_a significantly affected both unilateral and bilateral PDE, however, R significantly affected only unilateral PDE. The results showed that both models can be used to predict PDE, however, the nasal passage geometry information is easier to obtain than the resistance information.

Results of the mixed nonlinear regressions are shown below: (PDE = particle deposition efficiency, d_a = particle aerodynamic diameter, A_{min} = minimum nasal cross sectional area, E = nostril length/width ratio, and R=resistance)

The equations for bilateral deposition at a flowrate of 30 L/min are:

$$PDE_{Bilateral} = 1 - \exp(-0.08 * d_a^{1.43} * A_{min}^{-0.67} * E^{1.05}) \quad (n=40) \quad (1)$$

$$PDE_{Bilateral} = 1 - \exp(-0.06 * d_a^{1.56} * A_{min}^{-1.19} * E^{1.04}) \quad (n=23) \quad (2)$$

$$PDE_{Bilateral} = 1 - \exp(-0.12 * d_a^{1.47} * R^{0.30}) \quad (n=23) \quad (3)$$

The equations for unilateral deposition at a flowrate of 20 L/min are:

$$PDE_{Unilateral} = 1 - \exp(-0.14 * d_a^{1.43} * A_{min}^{-0.44} * E^{0.62}) \quad (n=80) \quad (4)$$

$$PDE_{Unilateral} = 1 - \exp(-0.10 * d_a^{1.50} * A_{min}^{-1.37} * E^{0.40}) \quad (n=46) \quad (5)$$

$$PDE_{Unilateral} = 1 - \exp(-0.04 * d_a^{1.51} * R^{0.93}) \quad (n=46) \quad (6)$$

Detailed methods and results are shown in the appendix in a manuscript submitted for publication. (Kesavanathan et al. The effect of nasal passage characteristics on particle deposition)

The Effect of Nasal Passage Characteristics on Particle Deposition in the Anterior Nasal Passage

The objective of this study was to determine the effects of nostril dimensions, nasal passage dimensions and nasal resistance (R) on the percentage of particle deposition in the anterior 3 cm of the nasal passage of spontaneously breathing humans. Forty healthy, nonsmoking subjects (aged 18 - 58 years) participated in the study. Male:female ratio was 26:14; African-American: Asian: European-American ratio was 21:4:15. The subjects inhaled through the nose a polydisperse 1-10μm diameter radioactivity tagged aerosol and exhaled through the mouth. A scintillation detector positioned in front of the nose measured radioactivity immediately post inhalation, then every two minutes for a total of 58 minutes. The detector, positioned laterally and collimated, also quantified regional activity at intervals from the nose to the pharynx at 42 - 48 minutes. At 52 minutes post deposition, a nose wipe removed activity from the accessible anterior nasal passage. After wiping the anterior nasal passage, a "post-wipe activity" was measured at 58 minutes. Minimum nasal cross sectional area (A_{min}) ranged from 0.24 - 1.29 cm^2, while R ranged from 1.06 - 8.29 cm H_2O/l/sec. Nasal length-width ratio (Ellipticity, or E) ranged from 0.89 - 4.00. Significant ethnic differences occurred with nostril length, width, E, and angle. Anterior particle deposition correlated significantly with the nostril length and E, but not with R or A_{min}. A multiple regression using E and A_{min} showed that E significantly affects all 3 measurements of the anterior deposition. We conclude that nostril ellipticity, but not internal nasal passage dimensions, determines anterior nasal passage particle deposition. Detailed methods and results are shown in the appendix in a manuscript submitted for publication. (Kesavanathan et al. The effect of nasal passage characteristics on particle deposition in the anterior nasal passage)

Measurement of Local Deposition of 1-10 μm Particles in a Nasal Replicate Model

Little is known about the spatial distribution of deposited particles of any size in the nasal passage; this factor has a profound effect on the fate of deposited particles, whether they are expelled physically from the anterior nares, remain for an unspecified period in the vicinity of the nasal valve, or are rapidly cleared by the mucus flow beyond the anterior turbinate region. We have carried out studies with a replicate model of a human nasal passage made up of 3 mm coronal slices. Studies were carried out with three monodisperse aerosol with diameters of 2.0, 4.0, and 8.3 μm. The results of these studies are shown in Fig. 1, demonstrating a peak of deposition just posterior to the nasal valve. However, there is a detailed structure to the deposition pattern which is size dependent; the 2.0 μm aerosol has a double peak, while the larger and smaller size aerosols do not demonstrate such a behavior. The fractions shown in the figure are normalized to the total amount of aerosol mass deposited in the model, not to the amount of aerosol breathed; measurements and theory show that the percent deposition overall in this range of sizes increases with increasing particle diameter, reaching 100% at about 10 μm.

Comparison of Natural and Passive Methods for Measuring Nasal Deposition of Ultrafine Particles

Natural breathing and simulated breath-holding techniques have been used to measure inspiratory and expiratory head deposition of inhaled particles in human subjects. Because the simulated breath-holding path, in which the aerosol is drawn through the nose and mouth, differs from the natural path where inhaled particle enter the nose and penetrate through the larynx and trachea, the present study was under taken to compare the deposition of ultrafine aerosol between these two experimental methods. Two replicate human upper airway casts containing a nasal airway, an oral passage, and a laryngeal-tracheal section were used to measure the head deposition efficiencies of monodisperse silver or polystyrene latex particles. Particles whose thermodynamic diameters ranged from 3.6 to 150 nm were drawn through the casts at constant flow rates ranging from 4 to 30 L/min. For the inhalation study, test aerosols were drawn into the nasal airway and directed either through the laryngeal tracheal section or through the oral passage; these flow patterns were reversed for the exhalation study. Results indicated that the difference in ultrafine aerosol deposition was not statistically significant at the 95% confidence level between the nose-mouth and nose-trachea paths for inhalation ($p=0.10$) and exhalation ($p=0.33$). For the range of particle size and flow rates studied, this finding suggests that the simulated breath-holding method, where test aerosols are drawn through the nose and mouth, is appropriate for estimating the inspiratory and expiratory deposition efficiency of ultrafine particles in the nose-trachea path. This is an important finding for future studies, in that the passive method is simpler, more controllable, and does not require the use of substances such as radioisotopes. Detailed methods and results are shown in the appendix in a published manuscript . (Cheng et al. Deposition of ultrafine aerosols in the head airways during natural breathing and during simulated breath holding using replicate human upper airway casts)

Oral passage Deposition Studies in Replicate Models

Although mouth breathing is common while exercising, speaking, and singing, information on particles deposited in the oral airway during these activities is rather limited. In the present study, an experimental technique was proposed to measure the oral deposition of inhaled particles by using an external pump to draw test aerosols through the nose and mouth (passive method) and an oral extension tube. A replicate human upper airway cast was challenged with monodisperse particles ranging in size from 3.6 to 150 nm at constant flow rates of 7.5 to 30 L/min. For the inhalation study, test aerosols were drawn into the nasal cavity and directed either through the laryngeal-tracheal (L-T) section or the oral passage with/without the oral extension tube inserted up to uvula of the cast. These flow patterns were reversed for the exhalation study. Deposition efficiencies of inhaled particles in the main oral cavity were found approximately equal to those in the L-T section for both inhalation and exhalation. The results of analysis of variance showed that empirical measurements of particle deposition via the mouth-trachea path agreed well with the calculated oral deposition efficiencies based on the experimental data of aerosol intake via the nose-mouth path with/without insertion of the oral extension tube. The similarities between the empirical and calculated oral deposition suggest that the passive method combined

with an oral extension tube is appropriate for determining deposition efficiencies of ultrafine particles in the oral airway. This noninvasive method has potential application for determining the oral deposition of micrometer sized particles, which are often encountered in occupational environments.

Oral passage depositions were measured at cyclic and steady flow rates. A comparison of the results for the two methods of inspiratory breathing gave good agreement, suggesting that steady breathing is a satisfactory stimulant for real cyclic breathing for such diffusing particles breathed at such characteristic inspiratory conditions. Detailed methods and results are shown in the appendix in a manuscript submitted for publication. (Cheng et al. An experimental method for measuring deposition efficiency of ultrafine aerosols in human oral airways)

Calculation of Extrathoracic and Thoracic Deposition of Ultrafine Particles from 5-200 nm

Total deposition fraction during inspiration and expiration can be considered as an index of cumulative doses of inhaled particles. We have calculated the total deposition fraction of ultrafine aerosols from 5 to 200 nm in the extrathoracic airways and in the lung for two breathing rates, 7.5 and 15 lpm, based on the experimental data of total respiratory deposition measured by Schiller et al. (1988) and the empirical equations of extrathoracic airways developed by Cheng et al. (1993) and Swift et al. (1993). Our results indicated that the contribution of particle deposition during expiration to the total deposition fraction in the nasal and oral passages was important for particle size less than 20 nm. The total lung deposition fraction increased as particle size increased from 5 to 20 nm, and decreased consistently thereafter until particle diameter reached 200 nm. These trends were observed for both nasal and oral breathing regardless of respiratory flow rate. The effect of increase of flow rate was to decrease the total nasal deposition fraction and to increase the total lung deposition fraction for any given particle size. For flow rate equal to 7.5 lpm, the total nasal deposition fraction reached approximately 57% for 5 nm particles and decreased to only 3% for 200 nm particles. The contribution of nasal deposition during expiration was very significant for 5 nm particles; there was an increase of 20% deposition fraction during expiration in addition to the inspiratory deposition efficiency, 37%. The total lung deposition fraction was about 15% at 5 nm, reached 35% at 20 nm, and decreased down to 10% at 200 nm. For flow rate equal to 15 lpm, the total nasal deposition fraction was 44% for 5nm particles and 3% for 200 nm particles. The enhancement of nasal deposition fraction during expiration was 10% for 5 nm particles and only 1 to 3% for particles larger than 50 nm. The total lung deposition fraction was about 41% at 5 nm, rose up to 50% at 20 nm, and dropped down to 12% at 200 nm. Detailed methods and results are shown in the appendix in a manuscript submitted for publication. (Cheng et al. Calculation of total deposition fraction of ultrafine aerosols in human extrathoracic and thoracic regions)

Calculation of the Extrathoracic Dose from Typical Indoor Radon Progeny Size Distributions

Radon and thoron progeny are ultrafine particles in the size range of 1-200 nm, depending on whether or not they are attached to other aerosol particles. The diffusion coefficient of radon

progeny is a critical parameter in determining its dynamics while airborne. Depending on their diffusion coefficient and the breathing pattern of the subject, ultrafine particles have been shown to deposit in the nasal or oral airways. Substantial deposition in the head airways reduces the amount of radioactivity that deposits in the tracheobronchial tree. Thus, for accurate dosimetric calculations, it is important to know the deposition fraction of radon progeny in the head airways. Several adult head airway models were used to study the radon progeny deposition in human nasal and oral airways. Radon-220 progeny (^{212}Pb) were used in the study. The particle size as measured by a graded screen diffusion battery was between 1.2 and 1.7 nm, indicating that the particles were molecular clusters. Deposition was measured by collecting filter samples before and after the model and gamma counting the ^{212}Pb. Experiments were performed under the constant flow rates of 4-20 lpm. Deposition efficiencies were between 63% and 85% in the nasal airway and 48% and 78% in the oral airway. Previously reported deposition data in the same airway model for ultrafine particles between 4.6 and 200 nm and the deposition data of radon progeny were used to establish a turbulent deposition equation covering particle sizes from 1 to 200 nm, the entire size range for attached and unattached radon progeny. Detailed methods and results are shown in the appendix in a published manuscript (Cheng et al. Deposition of thoron progeny in human head airways)

Figure 1. Local Deposition of Inertial Particles in Nose Model

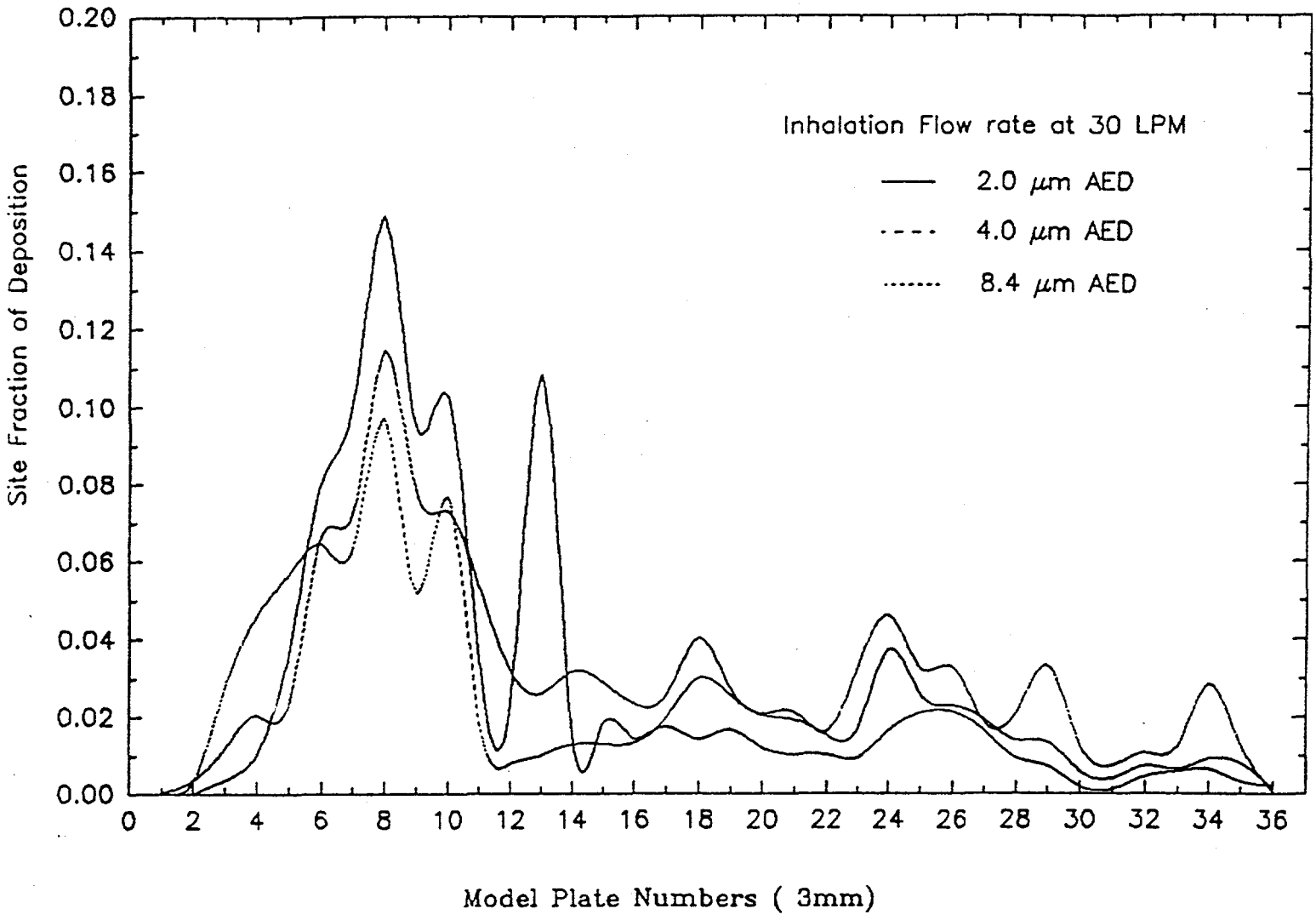

APPENDIX

The Effect of Nasal Passage Characteristics on Particle Deposition

Jana Kesavanathan, Ph.D.[1]
Rebecca Bascom, M.D., M.P.H.[2]
David L. Swift, Ph.D.[1]

[1] Division of Environmental Health Engineering, Department of Environmental Health Sciences, The Johns Hopkins University, School of Public Health, 615 N. Wolfe Street, Baltimore, Maryland 21205.

[2] Division of Pulmonary and Critical Care Medicine, University of Maryland School of Medicine, 10 South Pine Street, MSTF 800, Baltimore, Maryland 21201.

Running title: Nasal characteristics and particle deposition

Correspondence should be addressed to
Jana Kesavanathan
Room 6010
The Johns Hopkins University
615 N. Wolfe Street
Baltimore, MD 21205

ABSTRACT

This study determined the effect of nostril dimensions, nasal passage geometry, and nasal resistance (R) on particle deposition efficiency (PDE) in forty healthy, nonsmoking adults (24 male, 16 females) at a constant flowrate. An aerodynamic particle sizer measured the diameter and concentration of a polydispersed (1-10 μm diameter) aerosol drawn unidirectionally into the nose and out the mouth.

For each particle size, the concentration of particles entering the nose (C_{in}) and leaving the mouth (C_{out}) was measured. Nasal PDE, defined as $(C_{in}-C_{out})/C_{in}*100$, was calculated for bilateral and unilateral flow.

A mixed, nonlinear model was used to fit the PDE to two models based on two sets of specifications. The geometric model included particle aerodynamic diameter (d_a), nostril dimensions, and minimum nasal cross-sectional area (A_{min}); the resistance model included d_a and R. Left and right nasal passage PDE significantly correlated for 2-6 μm diameter particle sizes. The results showed that in both bilateral and unilateral geometric models, d_a, A_{min}, and E significantly affected PDE. In the resistance model, d_a significantly affected both unilateral and bilateral PDE, however, R significantly affected only unilateral PDE. The results showed that both models can be used to predict PDE, however, the nasal passage geometry information is easier to obtain than the resistance information.

INTRODUCTION

Inhalation is the major pathway by which workers and the general population are exposed to air pollutants. For nasal breathing, the typical human mode of breathing, the nasal passage is the first line of defense in the respiratory system. Particles filtered by the nasal passage do not reach the lung but may produce local effects in the nasal passage such as allergic responses. An understanding of the factors affecting PDE in the nasal passage will improve estimation of the delivered dose of toxic particles to the upper and lower respiratory tract.

Particles > 1 μm deposit in the nasal passage by impaction, a process influenced by particle aerodynamic diameter (d_a), air velocity, passage geometry, and changes in flow direction [1]. The effects of d_a and flowrate on PDE in the nasal passage have been studied extensively in humans and in replicate nasal casts. For a constant d_a, an increase in flowrate results in increased PDE [2,3], and for a constant flowrate, an increase in d_a results in increased PDE [3,4].

A few studies have evaluated the effect of nostril and nasal passage geometry on PDE in the human nasal passage. Rasmussen et al.'s [5] study showed that when the nasal passage is decongested, deposition increased. The authors did not control for flowrate and suggested that these increases might be due to an increased flowrate. A study conducted in our laboratory showed that decongesting the nasal passage does not affect PDE; however, enlarging and circularizing the nostril entrance significantly reduce deposition in the nasal passage suggesting that nostril dimensions could play an influential role within the nasal passage [6].

Most PDE equations include d_a and flowrate. Some studies, however, use pressure drop instead of flowrate in their deposition equations [2,7,8]. Cheng et al. [7] used other investigators' datasets to develop empirical nasal PDE equations for particles larger than 0.5 μm. They used two sets of variables: first set used particle size and flowrate and the second set used particle size and pressure drop.

Zhang and Yu [9] took the PDE modeling one step further by including anatomic features in the empirical PDE equation. They used previously published PDE equation and published average minimum nasal cross-sectional area (A_{min}) and average bend angle of the nasopharynx.

The objectives of the present investigation were to measure unilateral and bilateral PDE in ethnically diverse male and female human subjects, to evaluate the effect of nostril geometry, nasal

passage geometry, and nasal R on nasal PDE, and to model PDE by empirical equations. This study also evaluated the relationship between left and right nasal passage PDE.

MATERIALS AND METHODS

Subject Selection and Characterization

Forty healthy, nonsmoking adults aged 18 - 58 years participated in this study. African American (n=20), Asian (n=5), and European American (n=15) subjects participated in the study. Each subject's height, weight, age, and ethnicity were recorded and nostril entrance shape, nasal passage cross-sectional area, and nasal R were measured and recorded.

Nostril Shape

Nostril shape measurements included: (1) the major axis of the nostril cross section, (2) the minor axis of the nostril cross section, and (3) the angle of the major axis with the base of the nose (Figure 1). Then nostril length to width ratio (E) was calculated for each subject.

Acoustic Rhinometry

We used acoustic rhinometry (AR) to measures nasal passage cross sectional area as a function of distance from the nostril [10]. The AR method is as accurate as other methods in use such as magnetic resonance imaging and water displacement [10]. In addition, AR is a superior method for a study with a large subject population because it takes less than 30 seconds for each measurement and it does not require the subject to do any special maneuvers.

Jackson et al. [11] described the use of the AR to measure respiratory airway cross-

sectional area. Wear and Aki [12] and Sondhi and Resnick [13] have given theoretical background on this technique. Hilberg et al. [10] developed the system used in the present study, which is described in detail by Kesavanathan et al. [14].

Three measurements were taken of both the right and left side before and after the PDE measurements. A_{min}, anterior volume, middle volume, and posterior volume were determined from the AR measurements.

Posterior Rhinomanometry Measurement of Nasal Resistance

Rhinomanometry measures nasal R, defined as the ratio of the trans-nasal pressure drop to the flowrate. The method used in the present study was described in detail by Kesavanathan et al. [14]. Subjects wore a full face mask and breathed fast shallow breaths (nasal panting). Pressure and flow were measured continuously by transducers and were digitized for computer processing. R was determined from the expiratory limb, averaging the flows achieved at a pressure of 1 cm H_2O.

Posterior rhinomanometry measured nasal R before and after PDE measurements on subjects who were able to perform the nasal panting maneuvers. The nasal R was measured under three conditions: (1) both nasal passages (bilateral) open, (2) left nasal passage open and right nostril occluded, and (3) right nasal passage open, left nostril occluded.

Aerosol Generation

A high voltage electrospray method was used to generate polydispersed 1-10 μm diameter di-ethylhexyl sebacate aerosol in a 51 X 51 X 51 cm^3 plexiglass box [15]. The aerosol generating system is shown in Figure 2. Sixty-five percent (vol/vol) di-ethylhexyl sebacate in ethanol was fed by two needles kept at approximately 1.07 KV and 1.48 KV. The needles were positioned 90° to each other. A 9 KV negative electrode covered by a cylindrical shaped metal tube connected to ground was placed 7 cm in front of the 1.48 KV needles. Air at a flow rate of 30 L/min was

passed around the negative electrode inside the grounded cylinder. A ground electrode was placed 7 cm in front of the 1.07 KV needle. Particle aerodynamic diameter and concentration were measured with a TSI model 3310 aerodynamic particle sizer instrument (St. Paul, MN).

Particle Deposition Efficiency Measurements

Figure 3 shows the experimental system for measuring PDE. The aerosol was generated in a plexiglass box connected through a sampling port to the subject's nosepiece. The mouthpiece was connected through a sampling port to a vacuum pump. The subject took a deep breath closed his/her glottis before putting the nosepiece and mouthpiece in place. The vacuum pump then pulled the aerosol in through the nose and out the mouth. An aerodynamic particle sizer instrument measured particle size and concentration of aerosol entering the nose (C_{in}) and leaving the mouth (C_{out}). Nasal PDE was defined as $(C_{in}-C_{out})/C_{in}*100$ for each particle size.
Nasal PDE was determined under conditions of bilateral flow (30 L/min) and right and left unilateral flow (20 L/min).

Data Analyses

Subjects were grouped based on the basis of ethnicity. The nasal characteristics of subjects in each ethnic group were compared by ANOVA. African-American and European-American subjects' nasal characteristics were compared using a t-test. Nasal parameters were individually correlated with PDE of the nasal passage.

PDE for the left and right nasal passages of each subject was correlated for particle sizes of 2, 3, 4, 5, and 6 μm.

Mixed Non-linear Model

The mixed non-linear regression procedure is a SAS macro program written for applications involving the analysis of mixed effects nonlinear regression models for repeated measurements. It was written by Edward F. Vonesh (Baxter Healthcare Corporation, Round Lake, Illinois). The model which allow for both within and between subject heterogeneity has been useful in PDE applications [16].

Two kinds of nasal PDE models were fitted. The first used d_a, nostril dimensions, and nasal passage dimensions (geometry model), and the second used d_a and R (resistance model). Separate analyses were performed or bilateral and unilateral PDE. We were able to measure R in 23 of 40 subjects. For comparison reasons, the geometry model was also fitted with the same 23 subject.

RESULTS

Measurements of Nasal Geometry by Ethnicity

Table 1 shows nasal passage characteristics of subjects who participated in this study. Statistical analyses among the three groups showed that nostril width, E, and angle were significantly different among the three groups. A t-test showed that African American subjects had significantly different nostril width, E, and angle than European American subjects. The Asian subjects were not compared statistically with the other two groups due to their small number (n=5). Qualitatively, Asian group values tended to be intermediate between the other groups.

Measured Deposition Efficiency

Table 2 shows the nasal PDE. Values shown are percent average PDE for bilateral and unilateral nasal passages for 2 - 6 μm diameter particles with 30 L/min and 20 L/min constant flowrates,

respectively.

No significant correlation occurred when nasal parameters and other subject parameters were individually correlated with PDE of the nasal passage. Parameters that were individually correlated included nostril length, nostril width, E, nostril angle, A_{min}, anterior volume, middle volume, and posterior volume.

Mixed Nonlinear Regression

Results of the mixed nonlinear regressions are shown below: (PDE = particle deposition efficiency, d_a = particle aerodynamic diameter, A_{min} = minimum nasal cross sectional area, E = nostril length/width ratio, and R=resistance)

The equations for bilateral deposition at a flowrae of 30 L/min are:

$$PDE_{Bilateral} = 1 - \exp(-0.08 * d_a^{1.43} * A_{min}^{-0.67} * E^{1.05}) \quad (n=40) \qquad (1)$$

$$PDE_{Bilateral} = 1 - \exp(-0.06 * d_a^{1.56} * A_{min}^{-1.19} * E^{1.04}) \quad (n=23) \qquad (2)$$

$$PDE_{Bilateral} = 1 - \exp(-0.12 * d_a^{1.47} * R^{0.30}) \quad (n=23) \qquad (3)$$

Statistical analyses (Table 3) showed that d_a, A_{min}, and E significantly affected PDE in both equations (1) and (2), but that only d_a (but not R)significantly affected PDE in equation (3).

The equations for unilateral deposition at a flowrate of 20 L/min are:

$$PDE_{Unilateral} = 1 - \exp(-0.14 * d_a^{1.43} * A_{min}^{-0.44} * E^{0.62}) \quad (n=80) \qquad (4)$$

$$PDE_{Unilateral} = 1 - \exp(-0.10 * d_a^{1.50} * A_{min}^{-1.37} * E^{0.40}) \quad (n=46) \qquad (5)$$

$$PDE_{Unilateral} = 1 - \exp(-0.04 * d_a^{1.51} * R^{0.93}) \quad (n=46) \qquad (6)$$

Statistical analyses (Table 3) showed that d_a, A_{min}, and E significantly affected PDE in both equations (4) and (5), while both d_a and R significantly affected PDE in equation (6).

Figure 4 shows bilateral nasal PDE as a function of $d_a^{1.43} * A_{min}^{-0.67} * E^{1.05}$, Figure 5 shows bilateral nasal PDE as a function of $d_a^{1.56} * A_{min}^{-1.19} * E^{1.04}$, and Figure 6 shows bilateral nasal PDE as a function of $d_a^{1.47} * R^{0.30}$. Figure 7 shows unilateral nasal PDE as a function of $d_a^{1.43} * A_{min}^{-0.44} * E^{0.62}$, Figure 8 shows unilateral nasal PDE as a function of $d_a^{1.50} * A_{min}^{-1.37} * E^{0.40}$, and Figure 9 shows unilateral nasal PDE as a function of $d_a^{1.51} * R^{0.93}$.

Table 4 shows the correlation coefficient results for left and right unilateral PDE efficiencies of particles 2-6 μm. Left nasal passage deposition and right nasal passage deposition correlated significantly despite the large interindividual variation.

DISCUSSION

We collected data from male and female subjects of different ethnic background to develop equations which determine the percentage deposition of 1 - 10 μm diameter particles in the nasal passage. We confirmed the results of previous studies [17] indicating that nasal dimensions differ by ethnic group. Our results showed that nostril dimensions affect nasal PDE and support the use of demographically diverse populations in developing empirical equations for use. Previous studies used data from only Caucasian male subjects to develop the deposition equation and thus did not include a representative range of anatomic dimensions.

This study used the passive unidirectional flow method to measure PDE. An alternate method for measuring nasal PDE consists of a radioactivity tagged monodispersed aerosol that subjects inhale spontaneously through the nose, and exhale through the mouth. In the alternate method, a scintillation detector or gamma camera is used to measure the activity deposited in the nasal passage. It has been suggested that the passive method will overestimate the deposition in the nasal passage due to the sharp bend in the region of the oral-pharynx [5]. However a study by

Swift et al.[18], using a replicate nasal passage model, found no significant difference in deposition when aerosol passed in through the nose and out the trachea vs. in through the nose and out the mouth. We therefore consider our method to be representative of PDE under conditions of spontaneous breathing.

We used a flowrate of 30 L/min when aerosol was flowing through both nasal passages and 20 L/min when aerosol was flowing through one nasal passage. A ventilatory rate of 30 L/min is equallent to slight to moderate exercise. We found it to be the highest flowrate at which many of our subjects could reliably maintain a closed glottis during the passive breathing procedure. Our previous studies have shown that due to the nasal cycle, A_{min} of one nasal passage is typically twice as large as the other side. This suggests that the air flow occurs with a the ratio of 2 to 1(20 to 10 L/min) in the nasal passage. Nasal PDE is greater at higher flowrates, so we use 20 L/min in our unilateral PDE experiments.

Nasal PDE showed a large intersubject variation. No significant correlation was seen for deposition efficiency and many individual factors including nostril length, width, E, nostril angle, A_{min}, anterior volume, middle volume, R, age, height, and weight. Similar results were observed by Rasmussen [5] who measured deposition with 2.6 μm MMAD aerosol under conditions of spontaneous breathing.

Even though there is a large intersubject variability in deposition, left nasal passage deposition and right nasal passage deposition correlate well (Table 4). There have been no previous studies conducted to evaluate unilateral PDE in human subjects, but half nasal passage model deposition studies have been conducted by Itoh et al. [19] using different particle sizes and different gases. However, this model used only had one nasal passage; thus comparison between left and right nasal passage deposition could not be done.

Since many factors influence the impaction of particles [1], combining the factors as an

equation may be a good way of explaining PDE in the nasal passage. The geometric model shows that with the other parameters held constant the PDE increases as the d_a increases. In addition our study provides the new information that with the other parameters held constant PDE increases as E increases. E represents the shape of the nostril. A large E suggests an elliptical nostril while a close to 1.0 E suggests a round nostril. Therefore, PDE is greater when nostrils are elliptical shaped. We speculate that since nostril shape affects the anterior air flow pattern, this is the mechanism by which nostril shape affects PDE.

Another finding of the geometric PDE model was the inverse association between A_{min} and PDE; as A_{min} decreased, the PDE increased. We speculate that the increased PDE relates to increased turbulent flow which occures with decreased A_{min}. A study done by Zhang and Yu [9] also used an average A_{min} in the model.

In a study by Zhang and Yu nasopharynx angle was added to the PDE model in addition to A_{min}. They used nasopharynx angle since external nares information was not available. Their objective was to derive a mathematical form to facilitate interspecies comparison. Therefore, they used a published PDE equation and published average A_{min} and nasopharynx angle to create a PDE equation. Contrary to Zhang and Yu's objective, our objective was to derive a mathematical form to facilitate interpersonal comparisons. Therefore, we included each subject A_{min}, R, and E along with PDE information to develop PDE equations.

As shown above in results, this study modeled PDE with d_a, nostril dimensions and anterior nasal passage dimensions. Even after inclusion of these parameters in the model, there remains a large interindividual variation in deposition. This can be explained by Fry et al.'s (1973) study. Fry et al. evaluated the sites of particle deposition of 2-10 μm diameter particles in the human nasal passage and showed that 45 to 95% of the particles deposited in the nasal passage were in the anterior region, and the rest (5 to 55%) of the particles were deposited in the middle and posterior nasal passage. In our model, we included only anterior passage dimensions. The residual variation of deposition after fitting the model in our experiment may be due to the effect

of middle and posterior nasal passage dimensions.

The resistance model showed that as the d_a and R increases the deposition increases. R only affects the unilateral PDE significantly. The geometric and resistance models for bilateral (Equations 2 and 3) and unilateral (Equation 5 and 6) deposition showed that the dependence on d_a is very similar in the two equations. However, PDE modeling using geometry information is easier because AR measurements can easily be obtained on all the subjects compared to posterior rhinomanometry measurements.

Cheng et al. [7] used other investigators' datasets to develop empirical nasal PDE equations for particles larger than 0.5 μm. They also generated a geometric model and a pressure drop model. They had d_a and flow rate data from all studies, but pressure drop data were measured only in some of the studies. Cheng et al. reported that pressure drop equations gave slightly better correlations than the flow-based equation, however the constant values were quite different for each data set. The measured pressure drop was also different between subjects and for the same subject over time for the same flowrate [2].

In conclusion, the human nasal passage has a complex geometry and varying flow patterns. For these reasons, aerosol deposition in the nasal passage has been difficult to predict. New methods to measure posterior nasal passage geometry will improve particle deposition efficiency equations. At present, additional parameters which may influence PDE other than E and A_{min} are unknown. Future studies should evaluate the effect of middle and posterior nasal passage geometry in deposition.

Address reprint requests to:
Jana Kesavanathan
Room 6010
The Johns Hopkins University School of Public Health

615 N. Wolfe St.

Baltimore, MD 21205

LEGENDS

Figure 1. Illustration of the aerosol generating system.

Figure 2. Illustration of the nostril dimension measurements.

Figure 3. Illustration of the experimental setup for measuring particle deposition.

Figure 4. Nasal particle deposition in bilateral nasal passages at a flowrate of 30 L/min (n=40). $x = d^{1.43} * A_{min}^{-0.67} * E^{1.05}$ and y = deposition efficiency

Figure 5. Nasal particle deposition in bilateral nasal passages at a flowrate of 30 L/min (n=23).$x = d^{1.56} * A_{min}^{-1.19} * E^{1.04}$ and y = deposition efficiency

Figure 6. Nasal particle deposition in bilateral nasal passages at a flowrate of 30 L/min (n=23). $x = d^{1.47} * R^{0.30}$ and y = deposition efficiency

Figure 7. Nasal particle deposition in unilateral nasal passage at a flowrate of 20 L/min (n=80). $x = d^{1.43} * A_{min}^{-0.44} * E^{0.62}$ and y = deposition efficiency

Figure 8. Nasal particle deposition in unilateral nasal passage at a flowrate of 20 L/min (n=46). $x = d^{1.50} * A_{min}^{-1.37} * E^{0.40}$ and y = deposition efficiency

Figure 9. Nasal particle deposition in unilateral nasal passage at a flowrate of 20 L/min (n=46). $x = d^{1.51} * R^{0.93}$ and y = deposition efficiency

Reference

1. Hounam, R. F. and Morgan, A. 1977. Particle Deposition. *In* J.D. Brain, D.F. Proctor, and L.M. Reid, eds. Respiratory defense mechanisms (Part 1). Marcel Dekker, Inc, New York, 125-156.

2. Hounam, R. F., Black, A., and Walsh, M. 1969. Deposition of aerosol particles in the nasopharyngeal region of the human respiratory tract. Nature. 221:(5187):1254-1255.

3. Swift, D. L. 1991. Inspiratory inertial deposition of aerosols in human nasal airway replicate casts: implication for the proposed NCRP lung model. Radiation Protection Dosimetry. 38:(1/3):29-34.

4. Fry, F. A. and Black, A. 1973. Regional deposition and clearance of particles in the human nose. J Aerosol Sci. 4:113-124.

5. Rasmussen, T. R., Swift, D. L., Hilberg, O., and Pedersen, O. F. 1990. Influence of nasal passage geometry on aerosol particle deposition in the nose. Journal of Aerosol Medicine. 3:(1):15-25.

6. Nadarajah, S. and Swift, D. L. 1993. The Influence of cross sectional area on particle deposition in the human nasal passage. American Industrial Hygiene Conference. New Orleans, Louisiana (abstract)

7. Cheng, Y. S., Yeh, H. C. a., and Swift, D. L. 1991. Aerosol deposition in human nasal airway for particles 1nm to 20 μm:a model study. Rad Prot Dos. 38:(1/3):41-47.

8. Stahlhofen, W., Rudolf, G., and James, A. C. 1989. Intercomparison of experimental regional aerosol deposition data. Journal of Aerosol Medicine. 2:(3):285-308.

9. Zhang, L. and Yu, C. P. 1993. Empirical equations for nasal deposition of inhaled particles in small laboratory animals and humans. Aerosol Science and Technology. 19:51-56.

10. Hilberg, O., Jackson, A. C., Swift, D. L., and Pedersen, O. F. 1989. Acoustic rhinometry: evaluation of nasal cavity geometry by acoustic reflection. J Appl Physiol. 66:(1):295-303.

11. Jackson, A. C., Butler, J. P., Millet, E. J., Hoppin, F. G., and Dawson, S. V. 1977. Airway geometry by analysis of acoustic pulse response measurements. J Appl Physiol. 43:(3):523-536.

12. Ware, J. A. and Aki, K. 1968. Continuous and discrete inverse-scattering problems in a stratified elastic medium. J Accoust Soc Am. 11:911-921.

13. Sondhi, M. M. and Resnic, J. R. 1983. The inverse problem for the vocal tract: numerical methods acoustical experiments, and speech synthesis. J Accoust Soc Am. 73:(3):985-1002.

14. Kesavanathan, J., Swift, D. L., and Bascom, R. 1995. Nasal pressure-volume relationships determined with acoustic rhinometry. Journal of Applied Physiology. 79:547-553.

15. Nadarajah, S. and Swift, D. L. 1993. Generation of polydisperse aerosols of 0.5-10 micro meter diameter by electrospray. The American Association for Aerosol Research. Oak Brook, Il (abstract)

16. Vonesh, E. F. 1992, A SAS procedure for nonlinear mixed-effects models: Applied Statistics Center. Baxter Healthcare Corporation, Round Lake, IL. TR92M-0300,

17. Farkas, L. G., Hreczko, T. A., and Deutsch, C. K. 1983. Objective assessment of standard nostril types - a morphometric study. Annals of Plastic Surgery. 11:(5):381-389.

18. Swift, D. L. and Bickert, M. A. 1993. A comparison of methods to measure nasal filtration efficiency in vivo using a replicate human upper airway. American Association for Aerosol Research. Oak Brook, Illinois (abstract)

19. Itoh, H., Smaldone, G. C., Swift, D. L., and Wagner, H. N. 1985. Mechanisms of aerosol deposition in a nasal model. J Aerosol Sci. 16:(6):529-534.

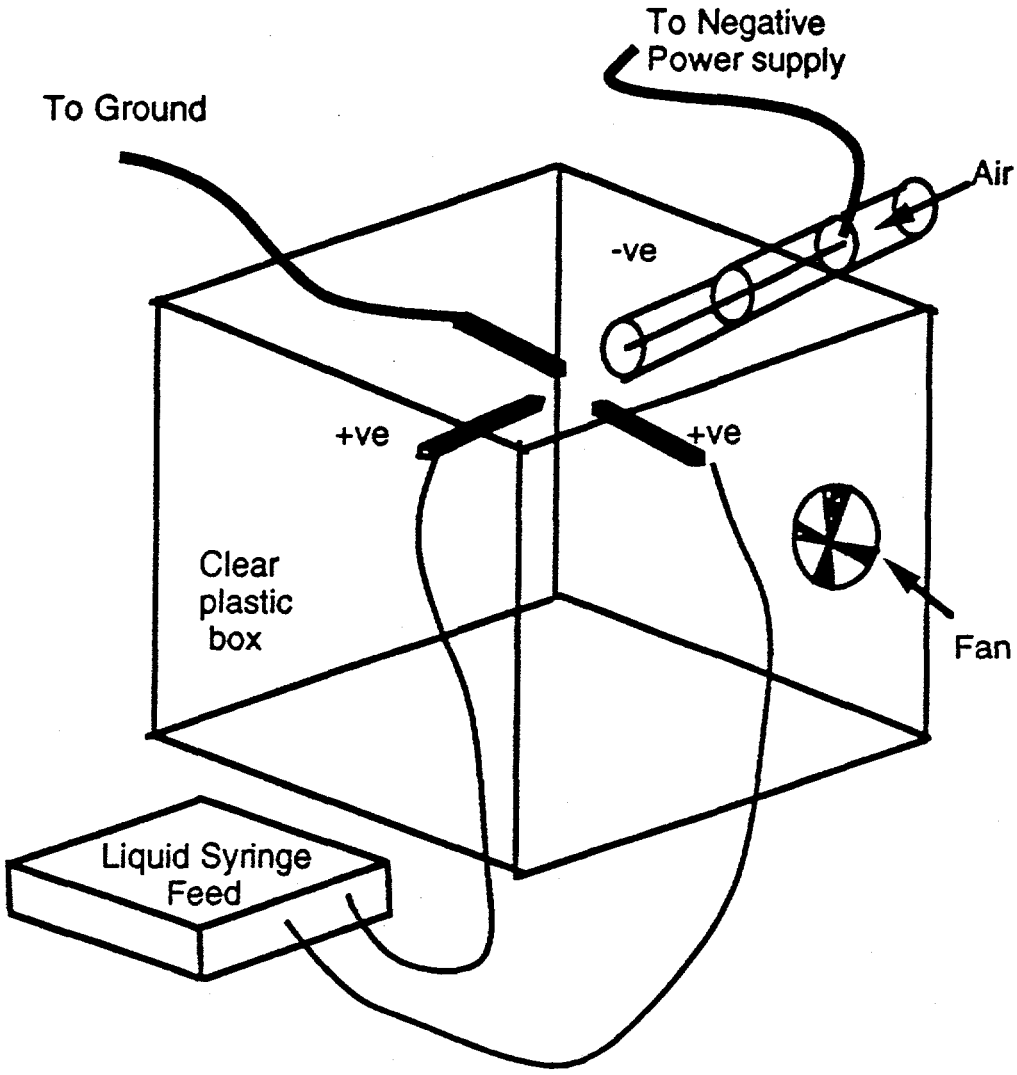

FIGURE 1. Aerosol Generating System

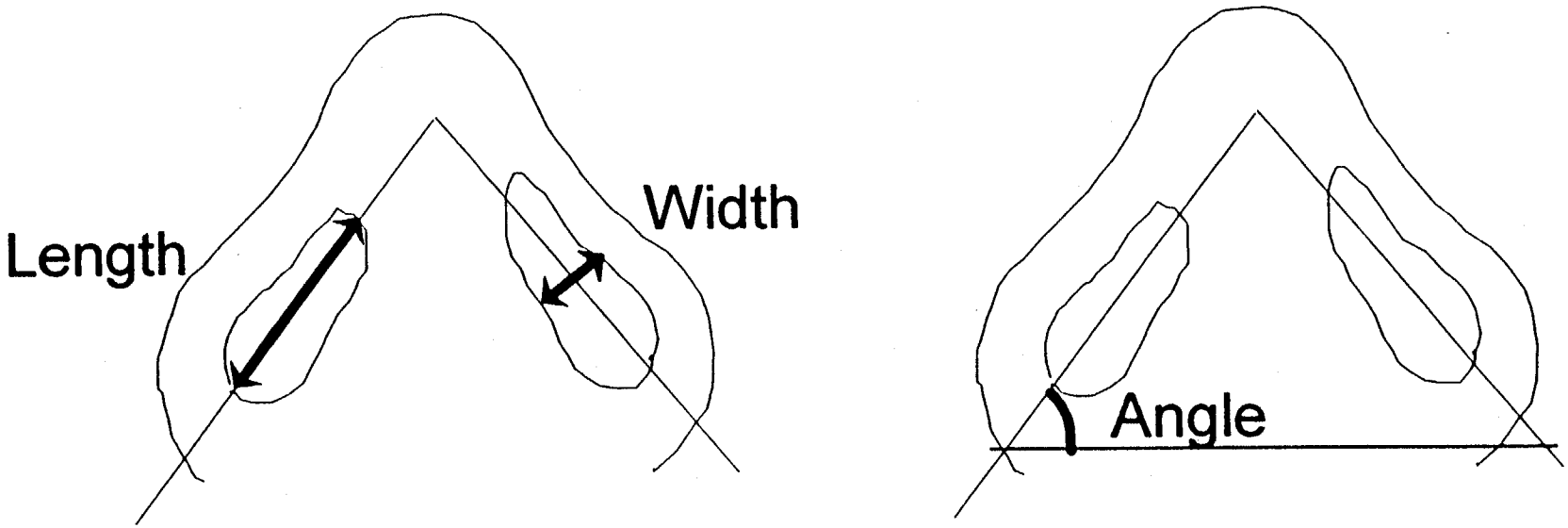

FIGURE 2.

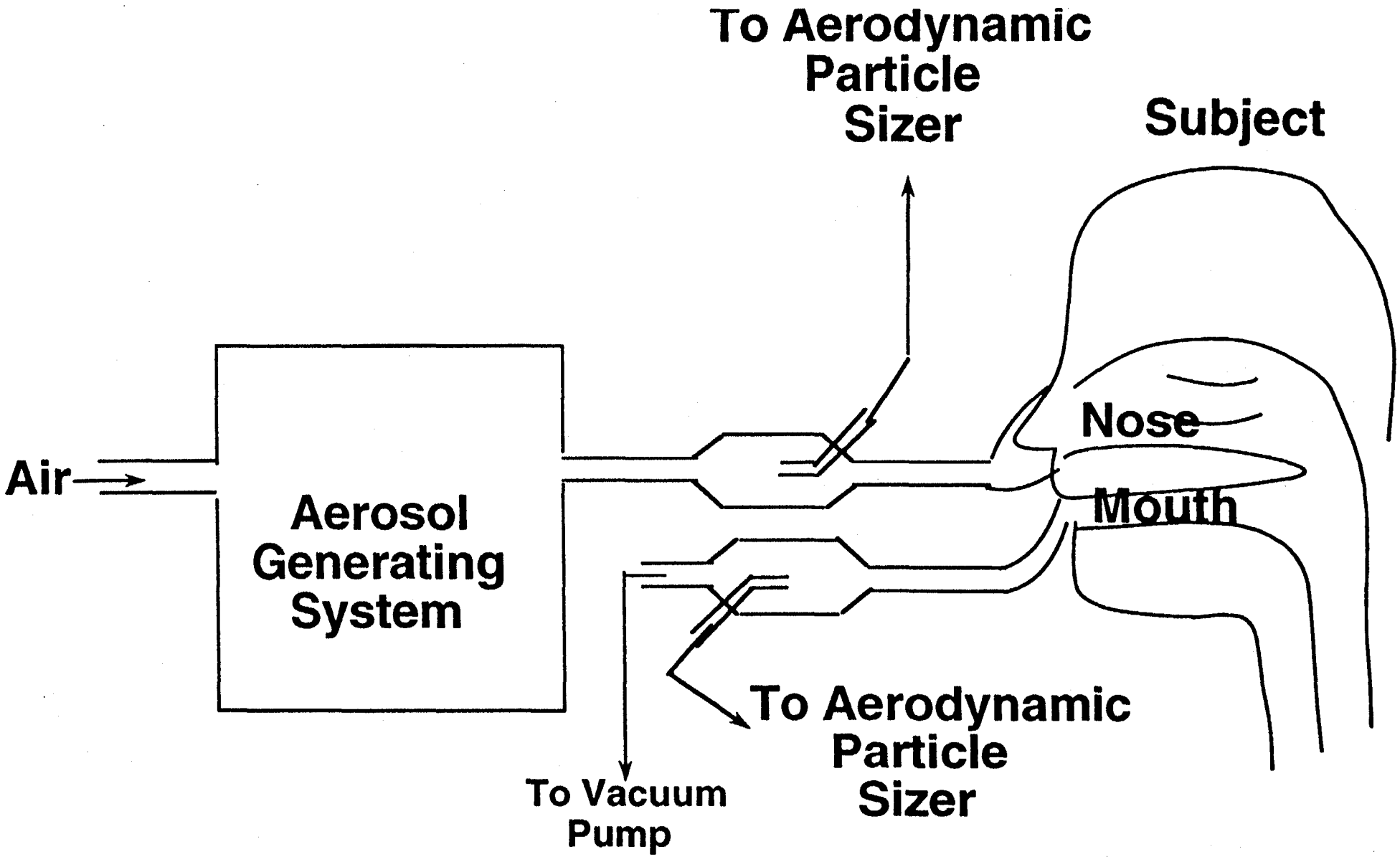

FIGURE 3: Experimental Setup

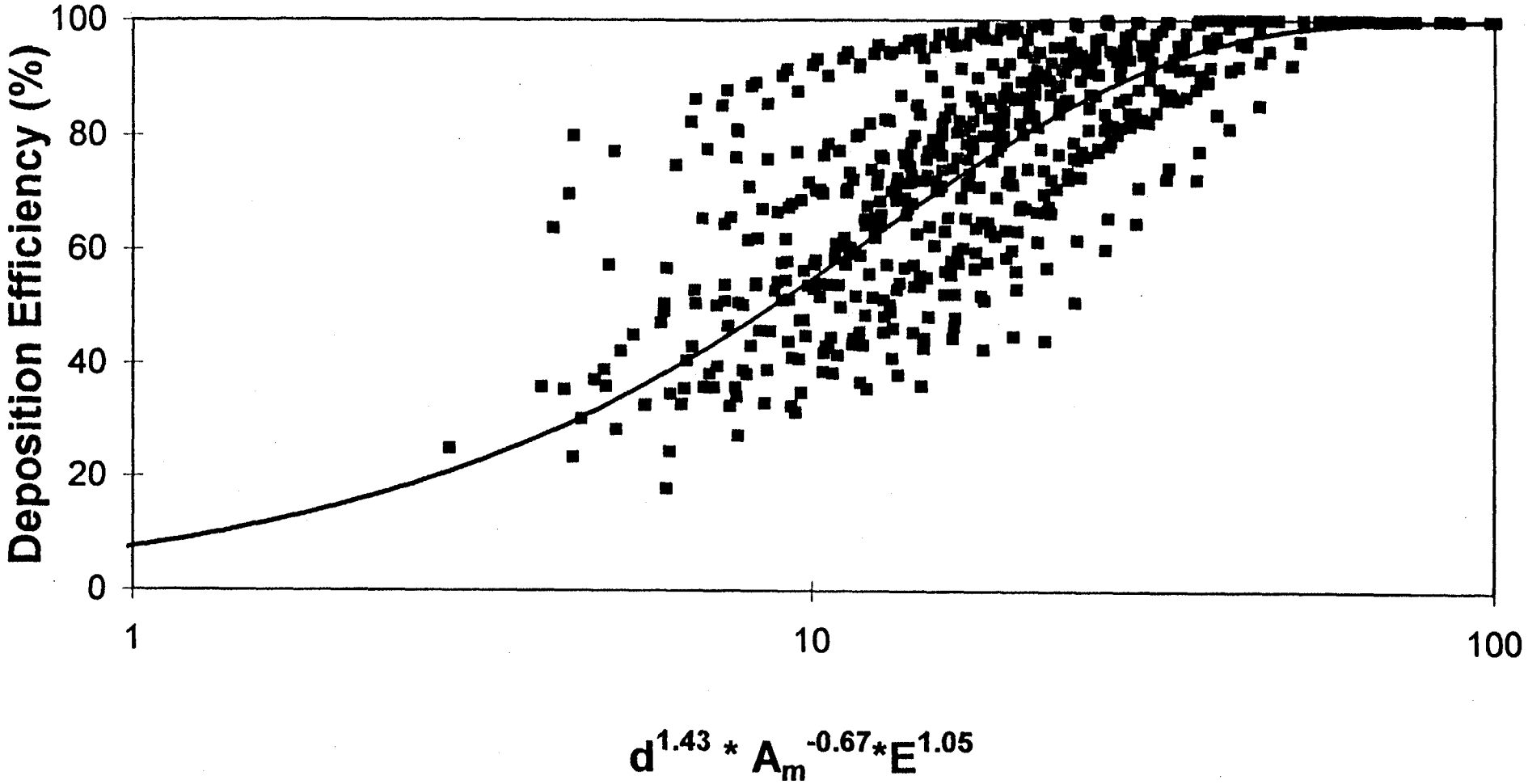

FIGURE 4. Bilateral Particle Deposition in the Human Nasal Passage (n=40)

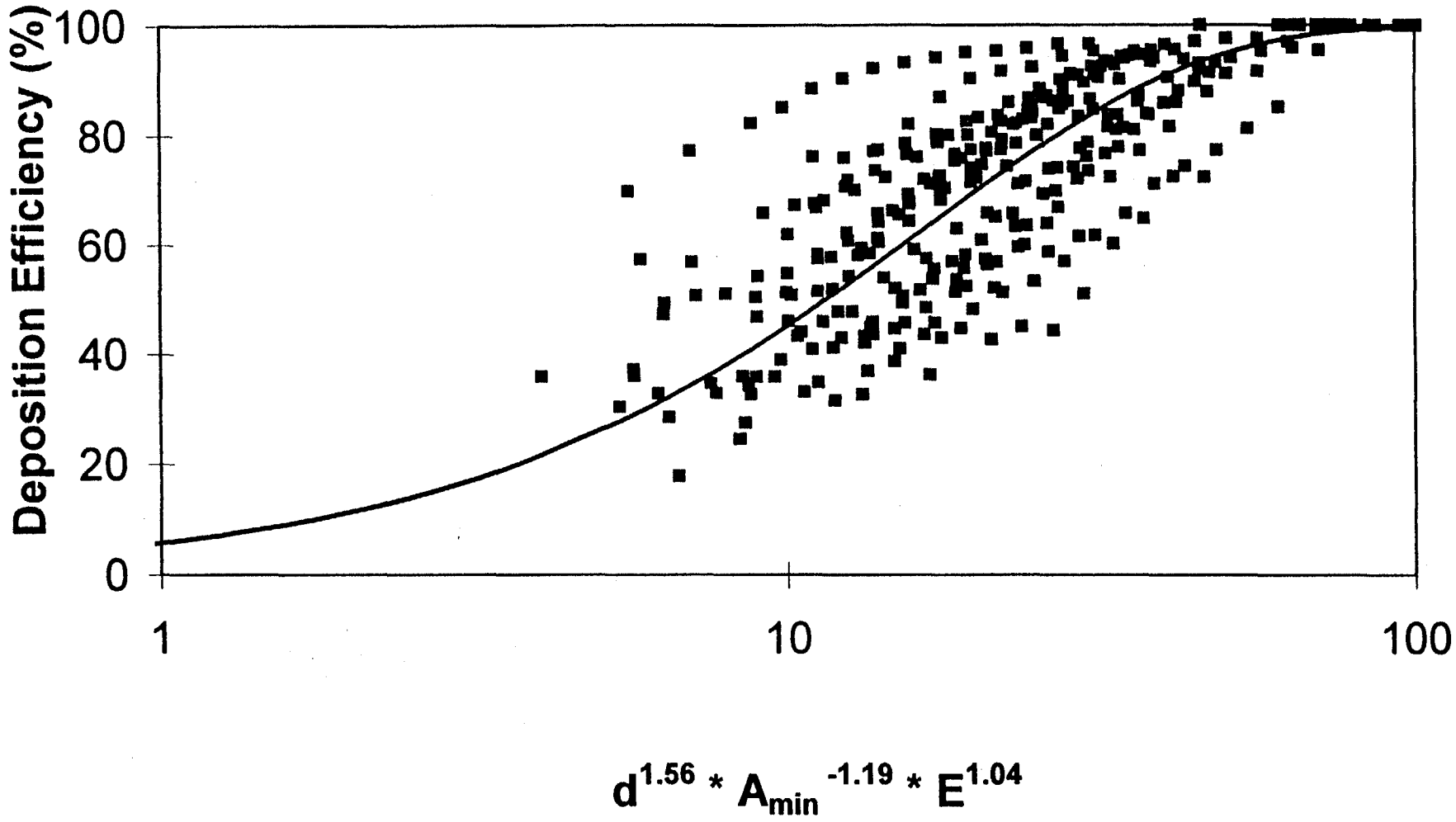

Figure 5. Bilateral particle deposition (n=23)

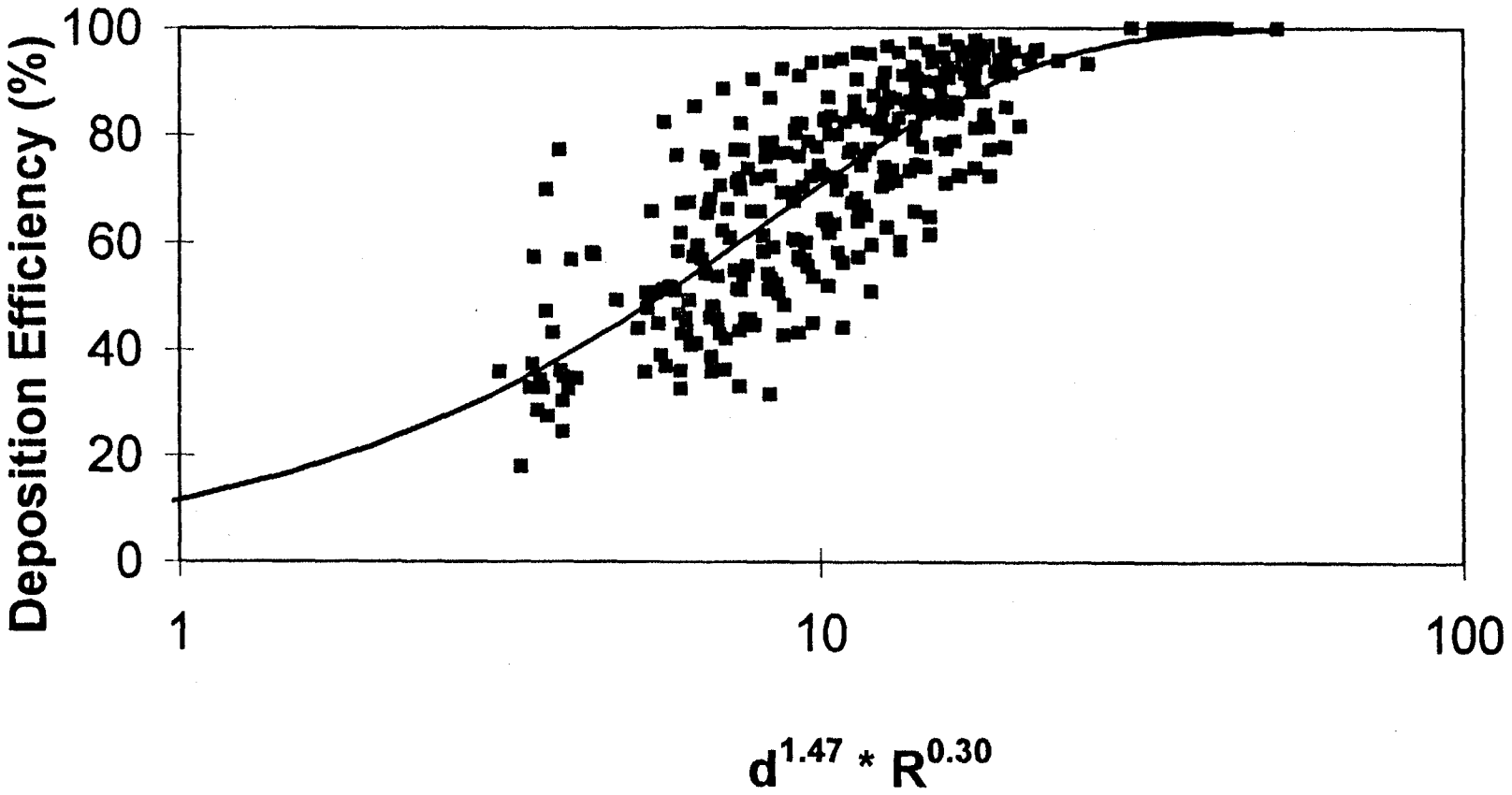

Figure 6. Bilateral particle deposition (n=23)

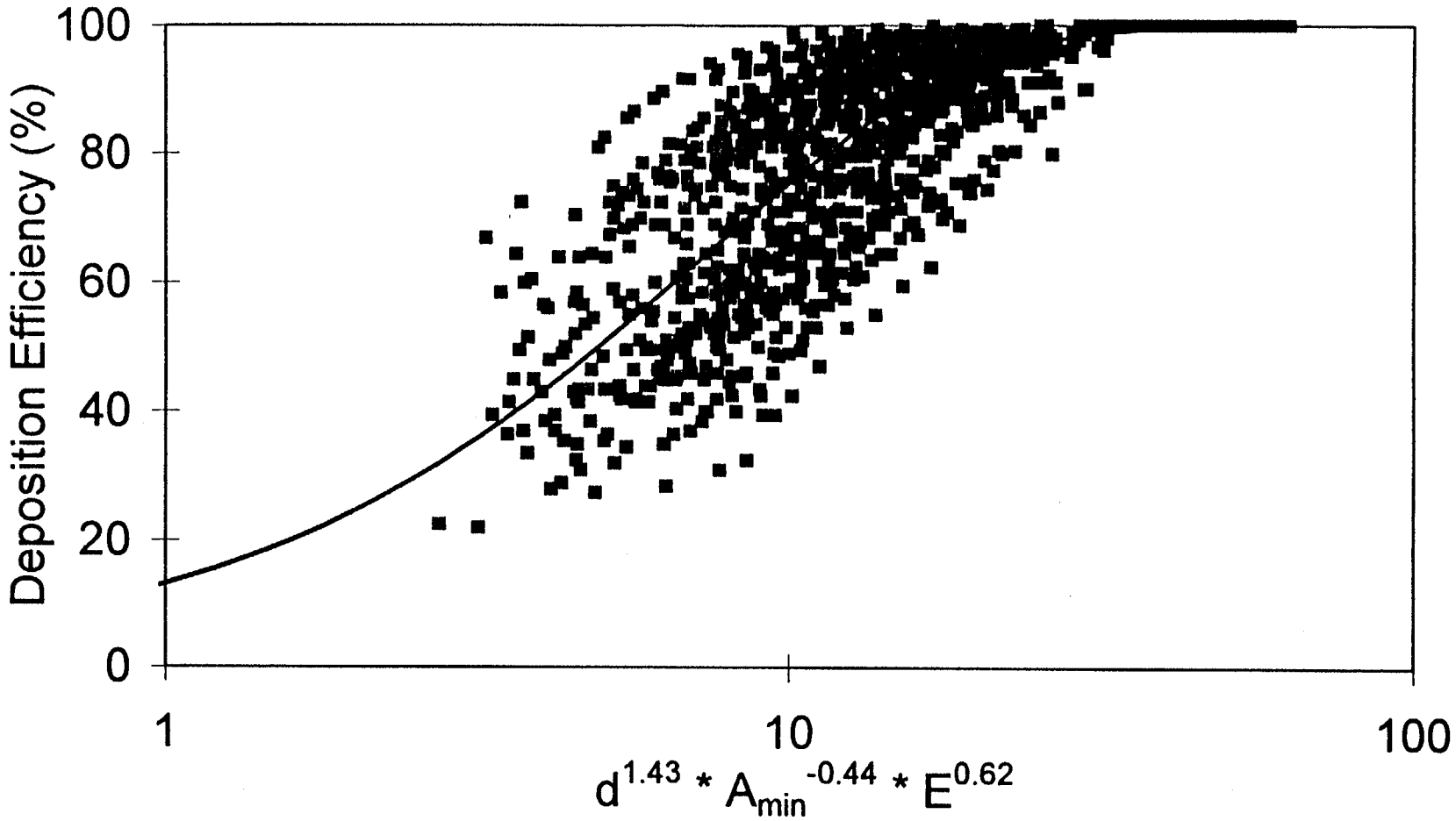

FIGURE 7. Unilateral Particle Deposition in the Human Nasal Passage (n=80)

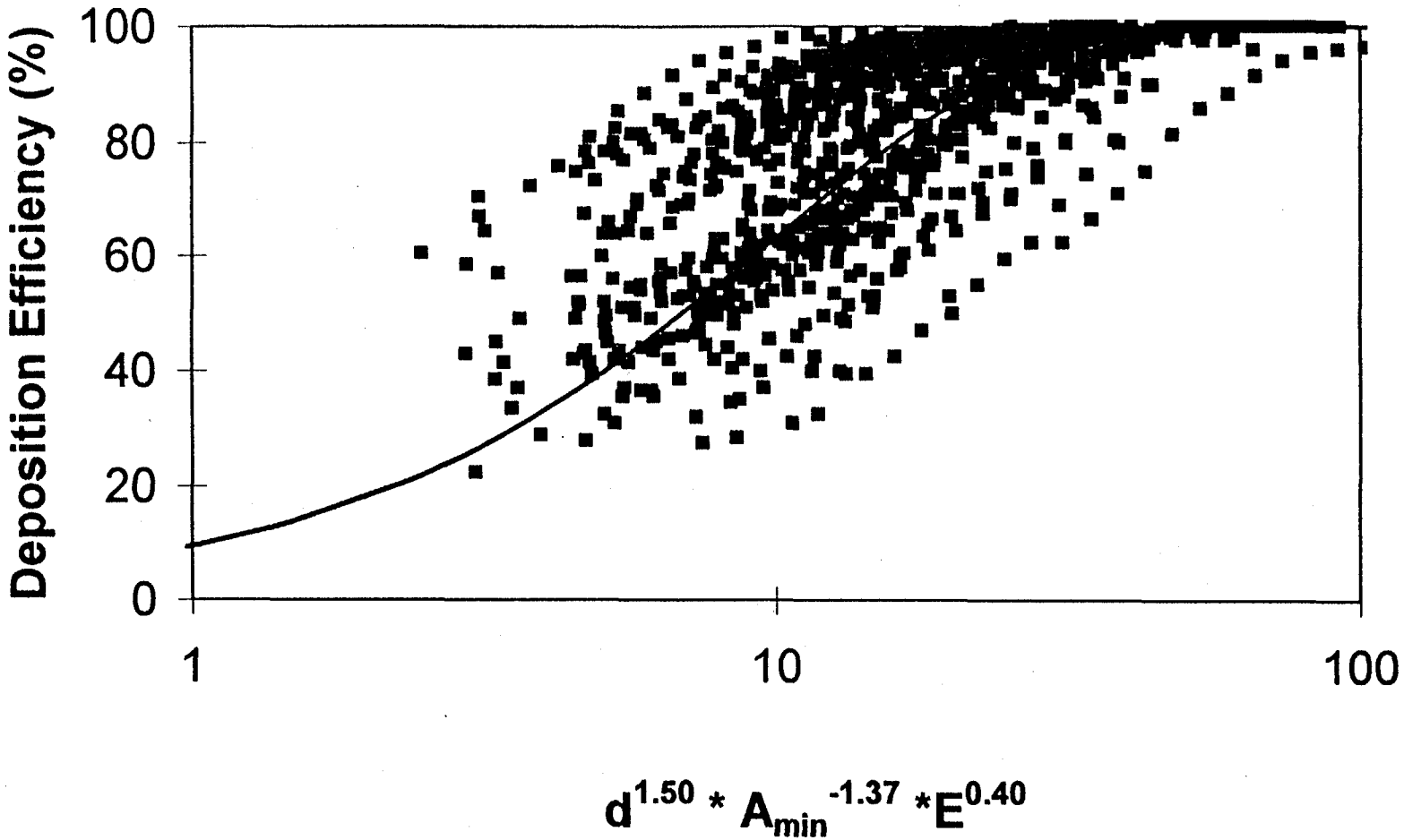

Figure 8.Unilateral particle deposition (n=46)

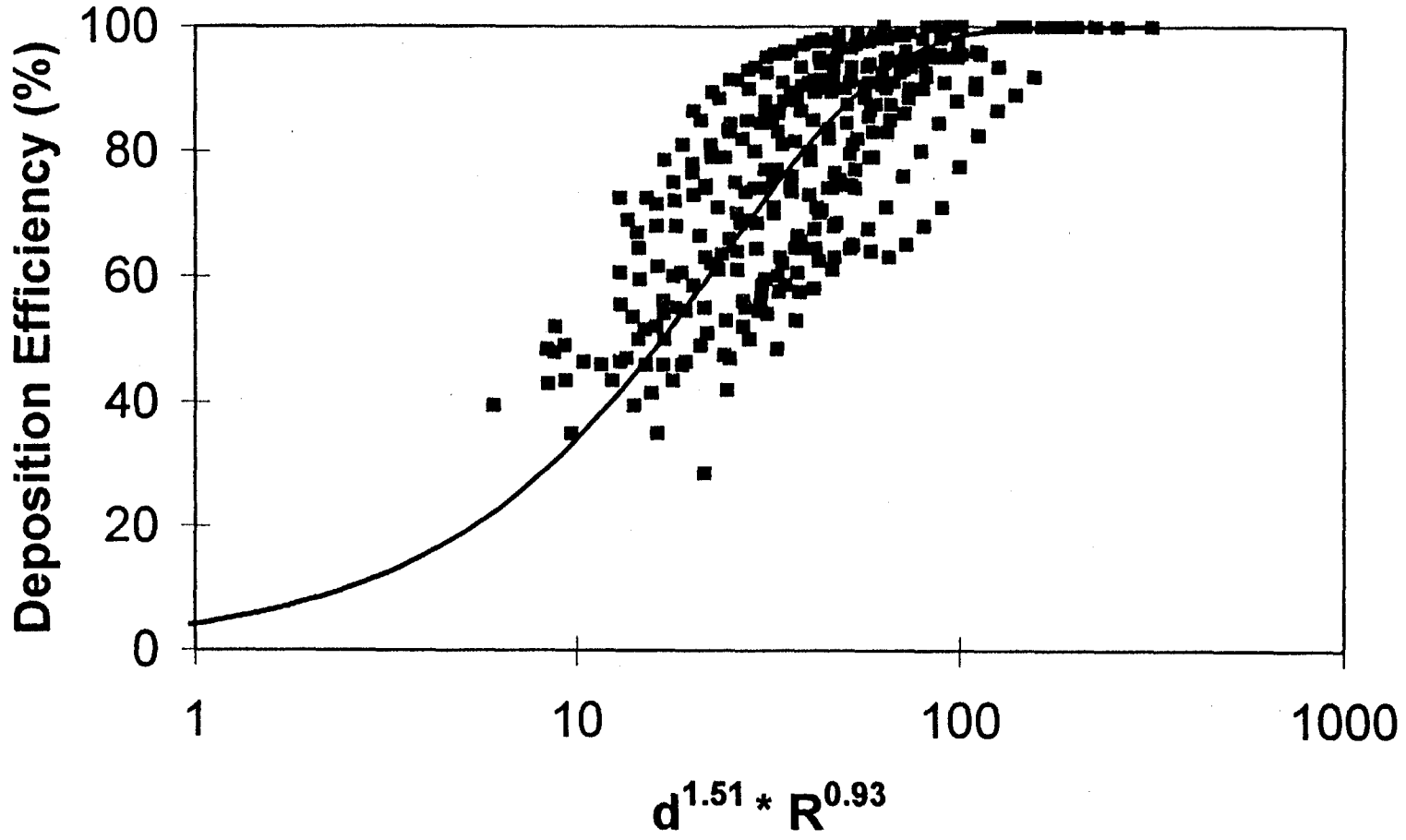

Figure 9. Unilateral particle deposition (n=46)

Table 1. Subject information grouped by ethnicity

	African American	Asian	European American
Gender (M:F)[a]	8:12	4:1	12:3
Age, years	32 (20 -43)	29 (22-32)	32 (18-58)
Nostril Dimensions			
Length, cm	1.58 (1.35-2.00)	1.55 (1.25-1.75)	1.71 (1.20-2.20)
Width, cm	1.03 (0.60-1.80)	0.85 (0.65-1.10)	0.80 (0.55-0.90)
Length/width ratio	1.60 (0.89-2.42)	1.89 (1.45-2.50)	2.14 (1.78-4.00)
Angle, degrees	24.2(14-35)	35.8(25-47)	51.2(37.5-65)
Nasal Passage Characteristics			
Minimum cross sectional area, cm^2	0.82(0.23-1.56)	0.75 (0.22-1.38)	0.79 (0.27-1.41)
Resistance (n=23), cm H_2O/l/sec	2.2(1.1-3.8)	2.6(1.6-4.4)	2.9(1.5-8.3)

All values are exprssed as mean (range)
[a] M = male, F = female

TABLE 2. Average bilateral and unilateral nasal particle deposition efficiency.

	2 μm	3 μm	4 μm	5 μm	6 μm
Bilateral (flowrate 30 L/min)	45±16	62±15	76±13	86±9	92±8
Unilateral (flowrate 20 L/min)	54±15	71±15	85±12	92±8	94±6

Values shown here are the mean±std, n=40
Bilateral = passive, unidirectional flow through both nasal passages simultaneously.
Unilateral = passive, unidirectional flow through one nasal passage at a time. Values shown here are pooled data separate measurements of the right and left nasal passages.

Table 3. Statistical results of nasal particle deposition models.
PDE = 1 - exp(k * d_a^d * A_{min}^a *E^e)--------model 1
PDE = 1 - exp(k *d_a^d * R^r)----------model 2

	n	k	d	a	e	r
Bilateral model 1	40	-0.08 **(p<0.0001)**	1.43 **(p<0.0001)**	-0.67 **(p<0.0015)**	1.05 **(p<0.0001)**	
Bilateral model 1	23	-0.06 **(p<0.0001)**	1.56 **(p<0.0001)**	-1.19 **(p<0.0001)**	1.04 **(p<0.0001)**	
Bilateral model 2	23	-0.12 **(p<0.0001)**	1.47 **(p<0.0001)**			0.30 **(p=0.1570)**
Unilateral model 1	80	-0.14 **(p<0.0001)**	1.43 **(p<0.0001)**	-0.44 **(p<0.0022)**	0.62 **p<(0.0005)**	
Unilateral model 1	46	-0.10 **(p<0.0001)**	1.50 **(p<0.0001)**	-1.37 **(p<0.0001)**	0.40 **(p<0.0045)**	
Unilateral model 2	46	-0.04 **(p<0.0001)**	1.51 **(p<0.0001)**			0.93 **(p<0.0001)**

TABLE 4. Correlation coefficient of left and right nasal passage deposition.

Particle Size (μm)	Correlation coefficient
2	0.50 ($p<0.05$)
3	0.63 ($p<0.05$)
4	0.62 ($p<0.05$)
5	0.53 ($p<0.05$)
6	0.56 ($p<0.05$)

The Effect of Nasal Passage Characteristics on Particle Deposition in the Anterior Nasal Passage

Jana Kesavanathan [1]

Rebecca Bascom [2]

David L. Swift [1]

[1]Division of Environmental Health Engineering, Department of Environmental Health Sciences, The Johns Hopkins University School of Hygiene and Public Health, Baltimore, Maryland, USA.

[2] Division of Pulmonary and Critical Care Medicine,
University of Maryland School of Medicine,
10 South Pine Street, MSTF 800, Baltimore, Maryland 21201.

Mailing Address
Jana Kesavanathan
US Army ERDEC
5232 Fleming Road
SCBRD - RTL E3150
Aberdeen Proving Ground, MD 21010
Phone: (410) 671-2073
Fax: (410) 612-7129

Abbreviated form of the title: Nasal characteristics and particle deposition

ABSTRACT

The objective of this study was to determine the effects of nostril dimensions, nasal passage dimensions and nasal resistance (R) on the percentage of particle deposition in the anterior 3 cm of the nasal passage of spontaneously breathing humans. Forty healthy, nonsmoking subjects (aged 18 - 58 years) participated in the study. Male:female ratio was 26:14; African-American: Asian: European-American ratio was 21:4:15. The subjects inhaled through the nose a polydisperse 1-10μm diameter radioactivity tagged aerosol and exhaled through the mouth. A scintillation detector positioned in front of the nose measured radioactivity immediately post inhalation, then every two minutes for a total of 58 minutes. The detector, positioned laterally and collimated, also quantified regional activity at intervals from the nose to the pharynx at 42 - 48 minutes. At 52 minutes post deposition, a nose wipe removed activity from the accessible anterior nasal passage. After wiping the anterior nasal passage, a "post-wipe activity" was measured at 58 minutes. Minimum nasal cross sectional area (A_{min}) ranged from 0.24 - 1.29 cm^2, while R ranged from 1.06 - 8.29 cm H_2O/l/sec. Nasal length-width ratio (Ellipticity, or E) ranged from 0.89 - 4.00. Significant ethnic differences occurred with nostril length, width, E, and angle. Anterior particle deposition correlated significantly with the nostril length and E, but not with R or A_{min}. A multiple regression using E and A_{min} showed that E significantly affects all 3 measurements of the anterior deposition. We conclude that nostril ellipticity, but not internal nasal passage dimensions, determines anterior nasal passage particle deposition.

Keywords: Ethnicity, particle deposition, nostril dimensions, and nasal passage dimensions

INTRODUCTION

The human extrathoracic airways are the first line of defense in the respiratory system [1]. Although some people breathe predominantly via the mouth, the nose is the more common route of inspiration, and particles filtered by the nasal passage may produce local injury.

The response of a region of the nasal passage to a toxic particle depends on the local dose, which is determined by the site of particle deposition and the rate and path of particle clearance. Particles which deposit inertially in the nasal passage are found predominantly in the anterior nasal passage [2,3] and the region of maximum deposition was previously reported to be approximately 2-3 cm posterior to the nostril [2]. This transitional region, located at the junction of the anterior squamous epithelium and the ciliated epithelium, is a common target for toxicant injury [4] and is the site of the nasal flow limiting segment, a key determinant of nasal resistance [5].

The site of particle deposition within the nasal passage will determine the mechanism of clearance and time-course of clearance. Particles deposited in the squamous or transitional epithelium, located at 0 - 2 cm posterior to the tip of the nose, are not cleared except by nose wiping, blowing or sneezing. Particles deposited in the anterior region of the ciliated epithelium (2 -3 cm) are cleared anteriorly by ciliary beating [6]. Particles deposited more posteriorly in the nasal passage are cleared toward the nasopharynx and swallowed [6]. Particles deposited in the nasopharyngeal region are also swallowed [7].

We previously empirically determined the total inhaled fractional deposition (PDE) in the human nasal passage in 10 subjects as a function of particle diameter (d, μm), flow rate (Q, l/min), minimum nasal cross-sectional area (A_{min}, cm^2), and nostril ellipticity, defined as the length-width ratio (E, unitless)[8]. In this equation, d, Q, A_{min}, and E significantly affect total particle deposition in the nasal passage.

$$PDE = 1 - \exp(-0.1 * d^{1.78} * (Q/100)^{1.12} * A_{min}^{-1.33} * E^{1.26})$$

The objective of this study was to determine the % anterior nasal passage particle deposition in spontaneously breathing human subjects as a function of nostril dimensions, nasal passage dimensions and nasal resistance. Spontaneous respiration was chosen over controlled flow rates because of our interest in predicting exposure dose relationships in occupational and environmental settings.

MATERIALS AND METHODS

Aerosol Generation

The aerosol generating system is shown in Figure 1. The principle of the high voltage electrospray method is that an electrically charged liquid bursts into an aerosol when emerging from a needle [9-13]. Varying the voltage alters the median aerodynamic diameter of the aerosol. Sixty-five percent (vol/vol) ^{99m}Tc sulfur colloid tagged di-ethylhexyl sebacate in ethanol was fed by two needles kept at approximately 1.07 KV and 1.48 KV and perpendicular to each other in a 51 X 51 X 51 cm^3 Plexiglass box. A 9 KV negative electrode, located inside a grounded cylindrical metal tube, was placed approximately 7 cm in front of the needles, and air at 30 l/min was directed towards the emerging aerosol. The negative electrode neutralized the charge on the particles. Approximately 7 cm in front of the 1.07 KV needle, a ground electrode was placed. The aerodynamic diameter was measured by a TSI model 3310 aerodynamic particle sizer (APS) (TSI Incorporated, St. Paul, MN).

Human Subjects

Forty healthy nonsmoking male and female subjects (26 male, 14 female) participated in this study. Subject characteristics are shown in Table 1. None of the subjects had significant nasal septal deviations as determined by acoustic rhinometry. An acoustic rhinometry system and posterior rhinomanometry system respectively measured nasal passage cross sectional area and nasal resistance.

Nostril Entrance Shape

The three nostril shape measurements were: (1) major axis of the nostril cross section (l), (2) minor axis of the nostril cross section (w), and (3) angle of the major axis with the base of the nose (Figure 2). The nostril ellipticity, defined as the length to width ratio and denoted E was calculated for each subject.

Acoustic Rhinometry

We used acoustic rhinometry to measure nasal passage cross sectional area as a function of distance from the nostril [14]. Jackson et al. [15] described the use of the acoustic technique to measure respiratory airway cross-sectional area and Wear and Aki [16] and Sondhi and Resnick [17] presented the theoretical background. Hilberg et al. [14] developed the system used in the present study and our use is described in detail in Kesavanathan et al. [18].

The acoustic rhinometry method is as accurate as other nasal cross-sectional area measuring methods such as magnetic resonance imaging and water displacement [14]. Acoustic rhinometry is a superior method for a study with a large subject population because it takes less than 30 seconds and does not require the subject to do any special breathing maneuvers. From the acoustic rhinometry output, one can determine the minimum nasal cross sectional area (A_{min}), an important characteristic of nasal flow and particle deposition.

Posterior Rhinomanometry

Rhinomanometry measures nasal resistance, defined as the ratio of the trans-nasal pressure drop to the flowrate. We use the technique termed posterior rhinomanometry because the pressure drop is measured from the nostril to the oropharynx. Our method has previously been described in detail [18].

The nasal resistance was measured, before aerosol inhalation, during three conditions: (1) both nasal passages (bilateral) open, (2) left nasal passage (left-unilateral) open, right nostril was closed with tape, and (3) right nasal passage open (right-unilateral), left nostril closed with tape. Twenty-three of the forty subjects were able to perform technically adequate maneuvers.

Aerosol exposure systems

Figure 3 shows the experimental setup for aerosol exposure and deposition in the nasal passage. A flexible close-fitting nosepiece, connected to the aerosol chamber, transported the aerosol to the nasal passage during a tidal inspiration, and a mouthpiece connected to a spirometer through a filter received the tidal exhalation. No directional valves were used, to avoid losses due to impaction. Subjects were instructed in the maneuver, and a continuous spirometric tracing verified correct directional breathing. The subject breathed the aerosol for about one minute, an interval previously determined to deposit activity at least five fold above background.

Activity measurements

Immediately after aerosol exposure the subject sat facing the scintillation detector with the nose placed in a reproducibly fixed position relative to the detector (figure 4). Thirty second counts of nasal activity were taken every 2 minutes for 40 minutes, a time when clearance typically plateaus. Between 42 and 48 minutes post exposure, the position of the detector was altered, and the regional distribution of activity remaining in the nasal passage was measured using a laterally positioned, collimated detector (figure 5). The detector was then replaced facing the subject, and counts were made at 50 and 52 minutes. At 52 minutes post exposure a moist tissue, placed over the little finger, wiped the accessible anterior region of the nasal passage. Activity remaining in the nasal passage after the nose wipe was measured at 54, 56, and 58 minutes.

Selection of end points

We chose to analyze several interrelated measures of anterior nasal deposition. Our rationale was that a robust determinant of anterior nasal deposition should be evident in many related measures.

We chose 3 frontal measures of anterior nasal deposition, and two lateral measurements comparing anterior to posterior activity. The three measurements from the frontal position were: (1) Percentage activity in the nasal passage at 52 minutes post-deposition, since the dominant

contributor to the recorded activity is the first 3 cm of the nasal passage. The activity recorded by the scintillation detector decreases with the square of the distance from the source.

(2) Percentage activity removed with the nose wipe. This is a direct, but likely incomplete measure of anterior deposition, since not all the anterior nasal passage is accessible with the finger.

(3) Percentage activity remaining after the nose wipe. This measures residual anterior activity that eluded the finger wipe.

The two lateral measurements were:

(4) Activity in the first 3 cm of the nasal passage, and

(5) Activity at 3-7.5 cm of the nasal passage.

The activity in the anterior 3 cm is unlikely to be removed so reflects deposition alone. The activity in 3 - 7.5 cm will be the net result of deposition and clearance.

Data Analyses

Subjects were grouped by ethnicity and the nasal characteristics were compared between groups by ANOVA. African-American and European-American subjects' nasal characteristics were compared using a t-test for the two groups, and for the males only.

Measured activity remaining in the nasal passage after initial deposition was corrected for background, decay and was normalized for initial count. Statistical analyses determined the effect of ethnicity, gender, nasal passage geometry, and resistance on each of the 5 measures of nasal deposition. Multiple regression analyses determined the effect of E and A_{min} on the five activity measurements. Other measures of nostril and nasal passage dimensions were excluded as they were related variables.

RESULTS

Nasal Characteristics of Study Population

The study population exhibited a wide range of nasal dimensions (Table 1). Nostril length ranged from 1.20 to 2.20 cm, nostril width ranged from 0.55 to 2.17 cm, E ranged from 0.89 to 4,

and nostril angle ranged from 14 to 65°. The African-American group had significantly different nostril dimensions from European-American subjects (Table 2). Asian subjects were not compared statistically with the other ethnic groups due to their small subject number (Table 2).

Minimum nasal cross sectional area A_{min} ranged from 0.24 to 1.14 cm^2 and nasal resistance ranged from 1.06 to 8.29 cm H_2O/l/sec. There was no difference between ethnic groups for these measures (Table 2).

T-tests comparing the nostril dimensions between African American male (N = 9) and European American male (N = 13) subjects showed significantly greater nostril width ($p < 0.03$), E ($p < 0.004$), and angle ($p < 0.0001$) in the African American males. Male (N = 9) and female (N = 12) African American subjects showed that only nostril angle ($p < 0.04$) was significantly different between the two groups. The small number of European American females (N = 2) prevented statistical analysis of this group.

Activity remaining in the nasal passage

Figure 6 shows a typical clearance graph. The activity decreased most rapidly over the first 15 minutes, then decreased more slowly until 52 min post exposure. The anterior nose wipe produced a sharp drop in activity at 52 minutes.

Table 3 shows the correlation of nostril dimensions, A_{min}, and resistance with the five clearance parameters. Nostril length and E correlated significantly with four out of five parameters: % activity 52 min post deposition, % activity removed with nose wipe, % activity in the first 3 cm of the nasal passage (all positive correlations), and % activity in the 3-7.5 cm of the nasal passage (a negative correlation). Nostril width statistically significantly correlated with two parameters: % activity 52 min post deposition and % activity removed with nose wipe. Nostril angle, A_{min}, and nasal passage resistance did not correlate with any of the parameters (Table 2). ANOVA analysis by ethnicity or gender and using the 5 deposition parameters showed no correlation of ethnicity or gender and anterior deposition (Table 4).

Multiple regression results

Multiple regression using E and A_{min} are shown in Table 5. E significantly affects % activity 52 min post particle deposition, % activity removed with nose wipe, % activity in the anterior nasal passage, and % activity in the posterior nasal passage. A_{min} did not affect any of the measurements.

DISCUSSION

This is the first study to evaluate the effect of nostril shape and nasal passage properties on anterior particle deposition. We show that nostril length, width, and ellipticity (E) significantly affect particle deposition in the anterior nasal passage. Fry and Black [2] measured the regional deposition in the human nasal passage using a monodispersed aerosol and 3 laterally positioned detectors. Their data showed that 45 - 95 % of all particles deposited in the nasal passage were in the anterior nasal passage. The distribution of deposition did not seem to depend upon either particle size or whether aerosol delivery occurred by a passive delivery system or by active breathing. Rasmussen et al.[19] using a polydisperse aerosol and a single detector showed that 70% of the particles (range: 31-92%) deposited in the nose were in the anterior nasal passage and could be removed with a wet tissue. The present study, which also used a polydisperse aerosol and a single detector, showed similar deposition percentage in the anterior nasal passage (42-99%). The availability of only one detector limited our ability to measure regional deposition. We have since measured regional deposition and confirmed Fry and Black's data [2].

In the present study, the detector was positioned anteriorly facing the nasal passage so that the measured activity derived from the anterior region. Activity decreases approximately as the inverse square of the distance to the detector, so that a tracer at 1 cm would appear as 9 fold greater than a similar quantity located at 3cm. We did not correct for the effect of distance in this study.

Itoh et al. [20] studied particle deposition in unilateral nasal passage models and showed that total particle deposition was due to changes in airflow direction and turbulent flow past the

nasal valve. Turbulent flow in the nasal passage is affected by A_{min} [20]. Our study results showed that A_{min} (average of right and left sides) does not affect the amount of anterior particle deposition. One possible explanation is that the detector counting activity more strongly from the anterior nasal passage. The other possible explanation is that people have well-defined nasal cycles and one side of the nasal passage is more open than the other side at any time [21]. To address this possibility, unilateral nasal deposition studies could be performed.

Nasal resistance also did not affect anterior particle deposition. Nasal resistance is caused by nasal valve area and the middle and posterior nasal passage areas, and the more posterior zones may not affect the amount of anterior particle deposition. While nasal resistance was not measured simultaneously with the deposition measurements, we believe it reflects nasal resistance at the time the particle deposition measurements were made.

This study was performed under conditions of spontaneous breathing. We previously showed that airflow affects total deposition and it likely affects regional deposition as well. However fixed flowrates do not reflect spontaneous breathing. When people breathe, the flowrate increases from zero to a variable maximum then back to zero, and both intersubject and intrasubject variation in breathing cycles are likely. Despite fixed total flowrates linear flow rates may differ in different regions of the nasal passage. We speculate that nostril shape and size affects the anterior air flow pattern and velocity resulting in different particle deposition patterns. Future studies using microanemometers could test this possibility.

Nostril ellipticity increases both total nasal particle deposition and the anterior nasal particle deposition. This reduces, on average, the dose of to toxic particles to the lower respiratory tract, and may reduce adverse lung health effects from exposure to inhaled particles in people with elliptical nostrils.

Although, the different ethnic groups have statistically different nostril structures, ethnicity alone did not predict the % of anterior deposition. The power of the study to detect ethnic

differences was less (because of greater variance) than the power to detect difference due to nostril dimensions. Future studies should include a measurement of the distance from the nose tip to where the ciliated epithelium begins in the nasal passage since this affects the amount of clearance of deposited particles. At the time of the study, non invasive techniques were not available to make these measurements.

Reactivity and solubility of vapors are understood to be important determinants of the site of epithelial toxicity, and animal studies have demonstrated focal epithelial toxicity at sites in the nasal passage. We speculate that nostril shape is important for tissue dose and toxicity at the transitional epithelium and that people with elliptical nostrils will show greater anterior toxicity, possibly leading to nasal congestive disorders at the flow limiting segment. This study shows that the demographic factors of ethnicity is only a surrogate for ellipticity, the factors that truly alters exposure-dose relationships. As researchers try to model susceptibility to inhaled pollutants, determinants such as ellipticity can be identified in the population, enabling more precise models.

Reprint request to:
Jana Kesavanathan
USA ERDEC
SCBRD RTL E3150
5232 Fleming Road
Aberdeen Proving Ground, MD 21010-5423

LEGENDS

Figure 1: Schematic diagram of high voltage electrospray aerosol generating system.

Figure 2: Schematic diagram of nostril length, width, and angle measurements.

Figure 3: Schematic diagram of the experimental setup for depositing radioactivity tagged aerosol.

Figure 4: Schematic diagram of the setup for measuring radioactivity in the nasal passage..

Figure 5: Schematic diagram of the setup for measuring activity remaining in each region of the nasal passage.

Figure 6: A typical clearance graph.

REFERENCE

1. Andersen, I. and Proctor, D. F. 1982. The fate and effects of inhaled materials. *In* D.F. Proctor and I. Andersen, eds. The nose: upper airway physiology and the atmospheric environment. Elsevier Biomedical Press, New York, 423-455.

2. Fry, F. A. and Black, A. 1973. Regional deposition and clearance of particles in the human nose. J Aerosol Sci. 4:113-124.

3. Proctor, D. F., Andersen, I., and Lundqvist, G. 1973. Clearance of inhaled particles from the human nose. Arch Intern Med. 131:132-139.

4. Morgan, K. T. 1995. Nasal dorsimetry, lesion distribution, and the toxicologic patholigist: a brief review. *In* F.J. Miller, eds. Nasal toxicity and dosimetry of inhaled xenobiotics: implications for human health. Taylor & Francis, Washington, D.C. 41-57.

5. Cole, P. 1982. Upper respiratory airflow. *In* D.F. Proctor and I. Andersen, eds. The nose: upper airway physiology and the atmospheric environment. Elsevier Biomedical Press, New York, 163-189.

6. Proctor, D. F. and Andersen, I. 1976. Nasal mucociliary function in normal man. Rhinology. XIV:11-17.

7. Lippmann, M., Yeates, D. B., and Albert, R. E. 1980. Deposition, retention, and clearance of inhaled particles. British Journal of Industrial Medicine. 37:337-362.

8. Kesavanathan, J. and Swift, D. L. 1996, Human nasal passage deposition: the effect of particle size, flowrate, and anatomical factors: American Industrial Hygiene Conference and Exposition, (Abstract)

9. Nadarajah, S. and Swift, D. L. 1993. Generation of polydisperse aerosols of 0.5-10 micro

meter diameter by electrospray. The American Association for Aerosol Research. Oak Brook, Il:

10. Meesters, G. M. H., Vercoulen, P. H. W., Marijnissen, J. C. M. a., and Scarlett, B. 1990. A Monodisperse Aerosol Generator Using the Taylor Cone for the Production of 1um Droplets. J Aerosol Sci. 21:(Suppl.1):s669-s672.

11. Meesters, G. M. H., Vercoulen, P. H. W., Marijnissen, J. C. M. a., and Scarlett, B. 1992. Generation of Micron-Sized Droplet from the Taylor Cone. J Aerosol Sci. 23:(1):37-49.

12. Gomez, A. and Tang, K. 1994. Charge and Fission of Droplets in Electrostatic Sprays. Phys Fluids. 6:(1):404-414.

13. Fernandez de la Mora, J., Navascues, J., Fernandez, F., and Rossell-Llompart, J. 1990. Generation of Submicron Monodisperse Aerosols in Electrosprays. J Aerosol Sci. 21:(Suppl. 1):s673-s676.

14. Hilberg, O., Jackson, A. C., Swift, D. L., and Pedersen, O. F. 1989. Acoustic rhinometry: evaluation of nasal cavity geometry by acoustic reflection. J Appl Physiol. 66:(1):295-303.

15. Jackson, A. C., Butler, J. P., Millet, E. J., Hoppin, F. G., and Dawson, S. V. 1977. Airway geometry by analysis of acoustic pulse response measurements. J Appl Physiol. 43:(3):523-536.

16. Ware, J. A. and Aki, K. 1968. Continuous and discrete inverse-scattering problems in a stratified elastic medium. J Accoust Soc Am. 11:911-921.

17. Sondhi, M. M. and Resnic, J. R. 1983. The inverse problem for the vocal tract: numerical methods acoustical experiments, and speech synthesis. J Accoust Soc Am. 73:(3):985-1002.

18. Kesavanathan, J., Swift, D. L., and Bascom, R. 1995. Nasal pressure-volume relationships determined with acoustic rhinometry. Journal of Applied Physiology. 79:547-553.

19. Rasmussen, T. R., Swift, D. L., Hilberg, O., and Pedersen, O. F. 1990. Influence of nasal passage geometry on aerosol particle deposition in the nose. Journal of Aerosol Medicine. 3:(1):15-25.

20. Itoh, H., Smaldone, G. C., Swift, D. L., and Wagner, H. N. 1985. Mechanisms of aerosol deposition in a nasal model. J Aerosol Sci. 16:(6):529-534.

21. Eccles, R. 1978. The central rhythm of the nasal cycle. Acta Otolaryngol. 86:464-468.

Table 1. Individual subject's nasal and activity measurements

			Activity measured at the face			% Regional Activity	
Demographic	A_{min} cm^2	E*	% Activity at 52 min	% Activity removed with nose wipe	% Activity in the nose after the nose wipe	Anterior	Posterior
1 BM**	0.91	1.45	63.50	45.10	18.20	47.80	52.20
2 BF	0.92	1.55	66.20	28.60	36.40	29.50	70.40
3 BF	0.24	1.56	49.40	33.00	14.70	75.50	24.40
4 BM	0.78	1.36	73.40	26.50	47.70	20.80	79.20
5 BF	0.92	1.57	61.60	31.90	31.50	57.20	42.80
6 BF	0.82	1.22	51.60	17.60	35.10	21.60	78.30
7 BF	0.71	1.29	73.80	29.50	44.10	35.60	64.40
8 BF	0.79	1.52	50.60	17.00	31.10	60.00	40.00
9 BM	0.98	1.40	52.20	30.90	22.10	64.80	35.10
10 BF	1.14	1.48	76.70	18.40	52.90	52.40	47.60
11 BF	0.52	1.65	69.30	33.10	33.30	58.50	41.40
12 BF	0.83	1.33	71.00	45.00	26.60	69.30	30.80
13 BM	0.79	1.83	87.40	46.90	43.30	61.50	38.40
14 BF	1.08	1.50	63.90	29.30	32.80	52.60	47.40
15 BF	0.87	1.25	65.40	32.70	33.90	40.80	75.20
16 BM	0.90	1.89	69.20	46.20	24.50	56.80	43.40
17 BM	0.59	2.17	57.40	32.20	26.60	40.50	59.50
18 BM	0.69	1.94	87.10	12.90	77.20	41.30	58.80
19 BM	0.97	2.05	99.40	42.90	56.60	61.40	38.60
20 BF	0.87	2.42	78.20	26.60	48.40	51.00	49.00
21 BM	0.92	0.89	55.60	21.60	33.90	56.60	43.40
22 AM	0.75	1.60	59.40	33.50	26.60	47.50	52.60
23 AM	0.69	1.56	61.40	32.10	28.50	50.70	49.20

24 AM	0.75	2.35	75.40	35.80	39.50	55.10	44.80
25 AM	1.00	2.50	91.70	64.10	27.30	53.00	47.10
26 EF	0.83	1.78	59.70	30.90	29.50	41.10	58.90
27 EM	0.90	2.31	82.30	30.40	48.20	26.40	76.50
28 EM	0.69	2.00	61.40	35.00	27.60	67.20	32.80
29 EM	0.61	2.24	69.50	37.80	32.50	85.00	15.70
30 EM	0.88	1.88	85.50	30.40	60.30	25.50	74.00
31 EM	1.03	2.00	87.60	52.60	34.50	61.50	38.60
32 EM	0.54	2.09	99.00	49.00	59.20	99.00	1.00
33 EF	0.71	2.00	74.10	46.70	29.80	35.10	65.00
34 EM	1.03	2.44	75.00	36.90	38.50	71.00	29.00
35 EM	0.75	2.14	76.40	20.40	52.20	43.40	56.60
36 EM	0.92	1.88	53.40	24.40	31.60	43.60	56.40
37 EM	0.96	2.86	69.80	49.30	20.10	50.30	49.70
38 EM	0.72	2.18	68.10	33.00	38.00	60.50	39.60
39 EM	0.56	2.38	42.00	13.80	27.10	100.00	0.00
40 EM	1.29	4.00	79.90	51.60	29.70	100.00	0.00

* Ellipticity (nostril length to width ratio)

** B = African American, A = Asian, E = European American
M = Male, F = Female

Table 2. Subject characteristics grouped by ethnicity

	African American	Asian	European American
Gender(M:F)	9:12	4:0	13:2
Age, years	32(23-43)	29(22-32)	34(18-58)
Height	5.6(5.1-6.1)	5.8(5.7-6.0)	5.9(5.4-6.3)
Weight	164(87-260)	151(135-181)	159(120-205)
Nostril length, cm	1.58(1.35-2.00)*	1.55(1.25-1.75)	1.74(1.2-2.2)
Nostril width, cm	1.03(0.89-2.17)*	0.85(0.65-1.10)	0.79(0.55-0.90)
Nostril ellipticity	1.59(0.89-2.17)*	1.89(1.45-2.50)	2.25(1.78-4.00)
Nostril angle, degrees	24.5(14.0-35.0)*	33.0(25.0-40.0)	51.1(37.5-65.0)
Nasal resistance** cm H_2O/l/sec	2.49(1.06-4.45)	3.10(2.18-4.43)	3.01(1.59-8.29)
Average minimum nasal cross sectional area of left and right sides, cm^2	0.82(0.24-1.14)	0.80(0.69-1.00)	0.83(0.54-1.29)

The values shown in the table are mean(range)

* African American subjects are significantly different from Europian American subjects

** African American (M=5, F=5); Asian(M=3, F=0); European American (M=9, F=1)

Table 3. Correlation of activity measurements with nostril length, width, ellipticity, angle, A_{min}, and resistance (n=40).

Correlation	Length	Width	Ellipticity	Angle	A_{min}	Resistance
% activity in the nose at 52 min	0.26*	-0.32*	0.36**	0.09	0.25	-0.10
% activity Removed with nose wipe	0.36**	-0.28*	0.41**	0.23	0.21	0.03
% activity in the nose after nose wipe	-0.04	-0.10	0.03	-0.06	0.05	-0.09
% activity in the 0-3 cm segment of the nasal passage	0.40***	-0.20	0.42***	0.13	-0.11	0.19
% activity in the 3-7.5 cm segment of the nasal passage	-0.40***	0.22	-0.43***	-0.13	0.11	-0.19

*$p<0.05$; **$p<0.01$, ***$p<0.005$

Tabel 4. Nasal activity measurements grouped by ethnicity

	African American (n=21)	Asian (n=4)	Europian American (n=15)
% activity remaining in the nose after 52 min	67.8 + 13.2	72.0 + 15.0	72.3 + 14.5
% activity removed with nose wipe	30.9 + 10.1	41.4 + 15.2	36.2 + 11.8
% activity in the nose after nose wipe	36.7 + 14.4	30.5 + 6.1	37.3 + 12.2
% activity in the first 3 cm of the nose	50.3 + 14.3	51.6 + 3.3	60.7 + 26.1
% activity in 3-7.5 cm of the nose	50.5 + 15.7	48.4 + 3.3	39.3 + 26.3

The values shown in the table are mean $\pm$ std

Table 5 Multiple regression results

	Intercept	Ellipticity	A_{min}
% activity remaining in the nose after 52 min	44.09 $p < 0.0002$	8.02 $p < 0.045$	12.99 $p < 0.25$
% activity removed with nose wipe	12.5 $p < 0.16$	8.02 $p < 0.02$	7.6 $p < 0.41$
% activity in the nose after nose wipe	32.73 $p < 0.005$	0.49 $p < 0.90$	3.22 $p < 0.78$
% activity in the first 3 cm of the nose	40.81 $p < 0.008$	16.67 $p < 0.003$	-21.88 $p < 0.16$
% activity in 3-7.5 cm of the nose	60.25 $p < 0.0002$	-17.49 $p < 0.003$	23.05 $p < 0.15$

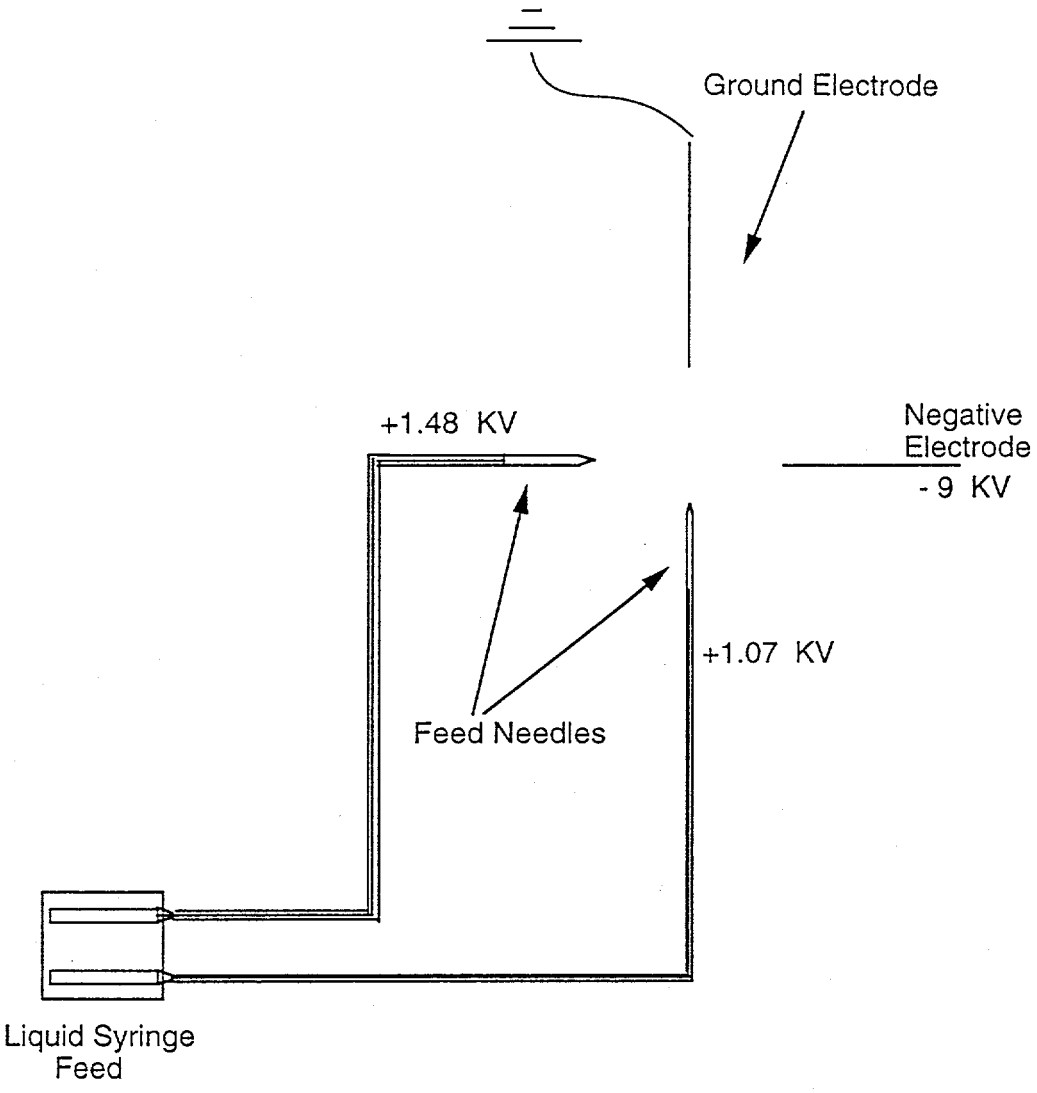
Ground Electrode
+1.48 KV
Negative
Electrode
- 9 KV
+1.07 KV
Feed Needles
Liquid Syringe
Feed

Figure 1.

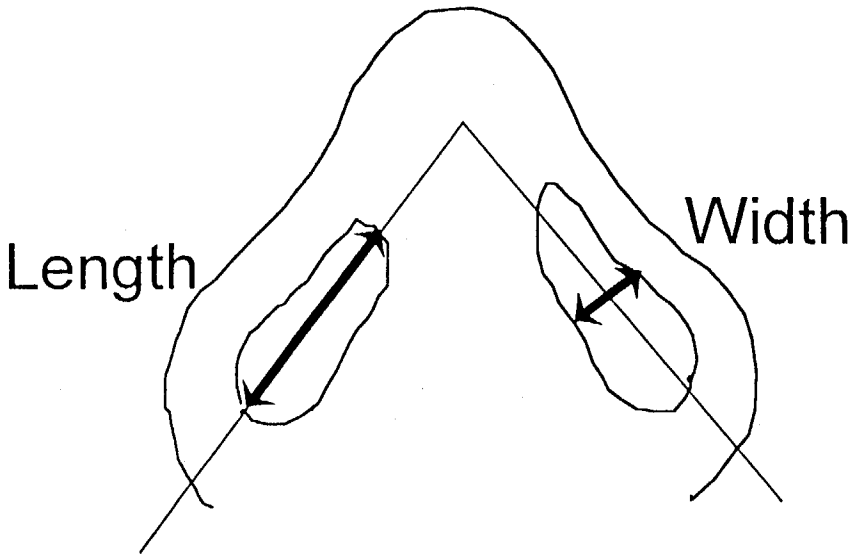

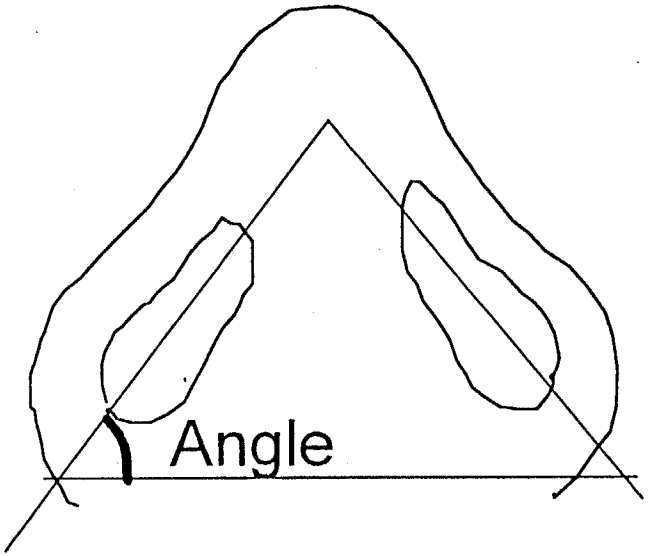

Figure 2

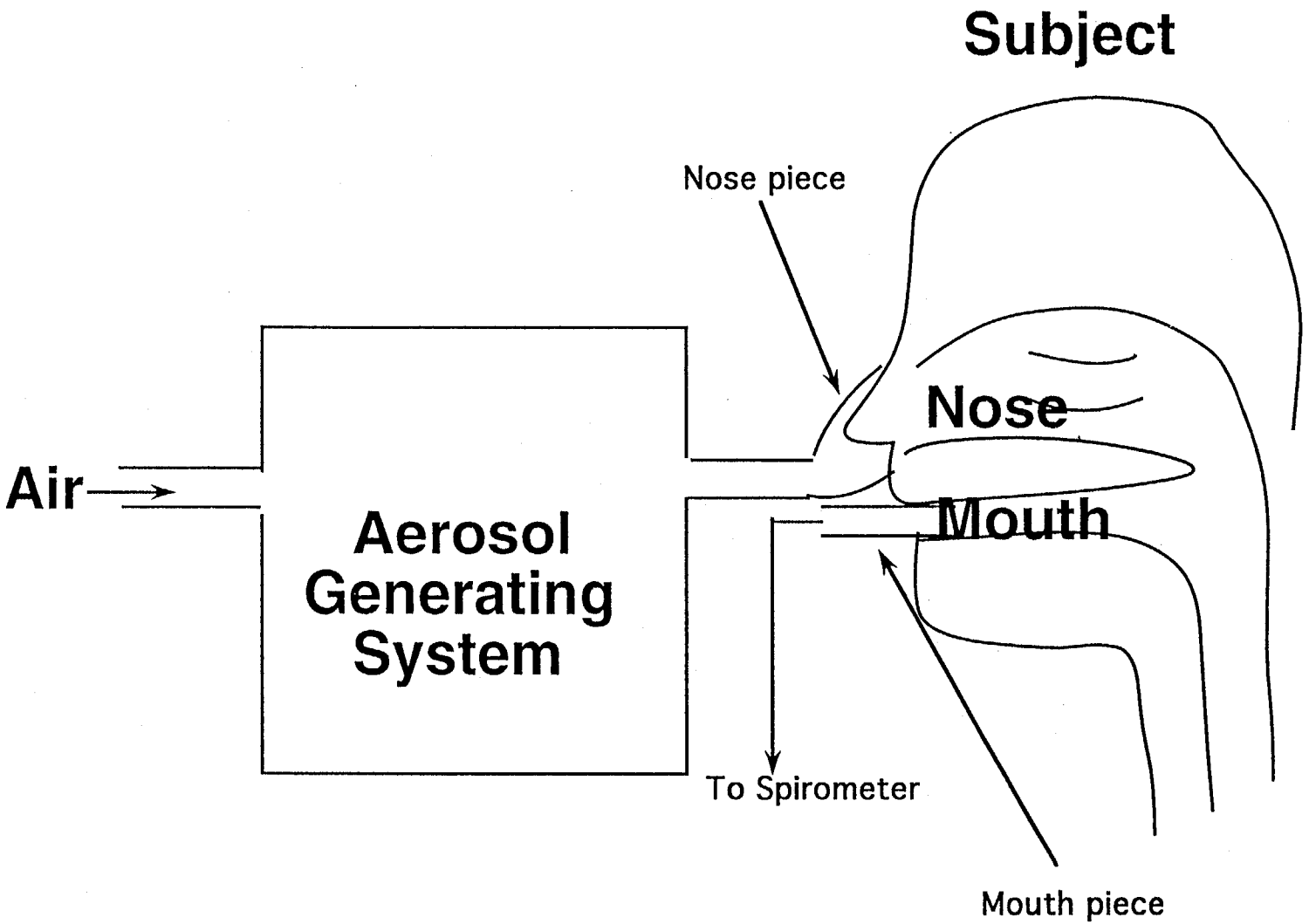

Figure 3. Experimental Setup

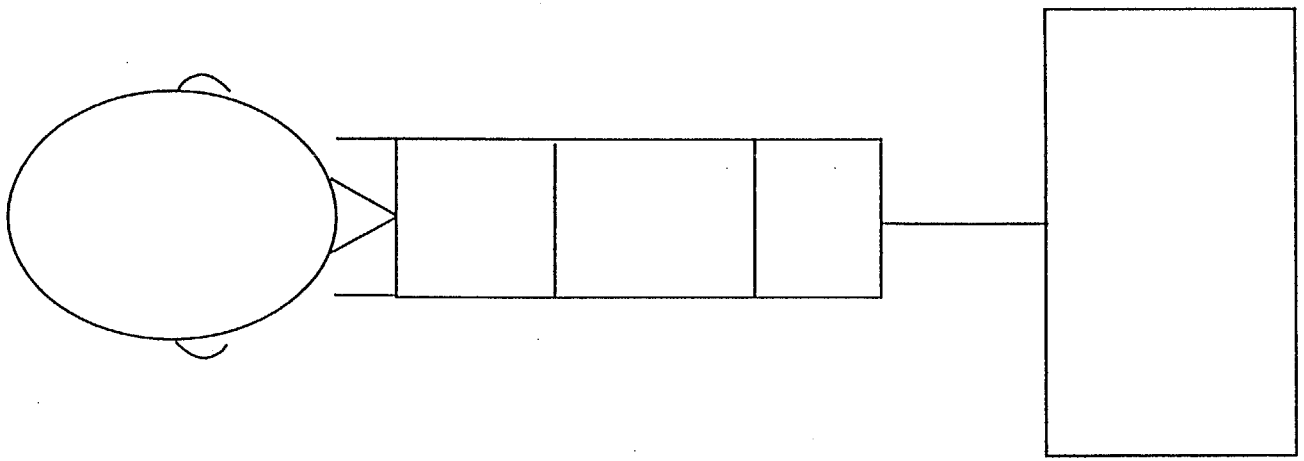
SUBJECT
SHIELDED
DETECTOR
SCALER-TIMER
HIGH VOLTAGE
POWER SUPPLY

Figure 4:

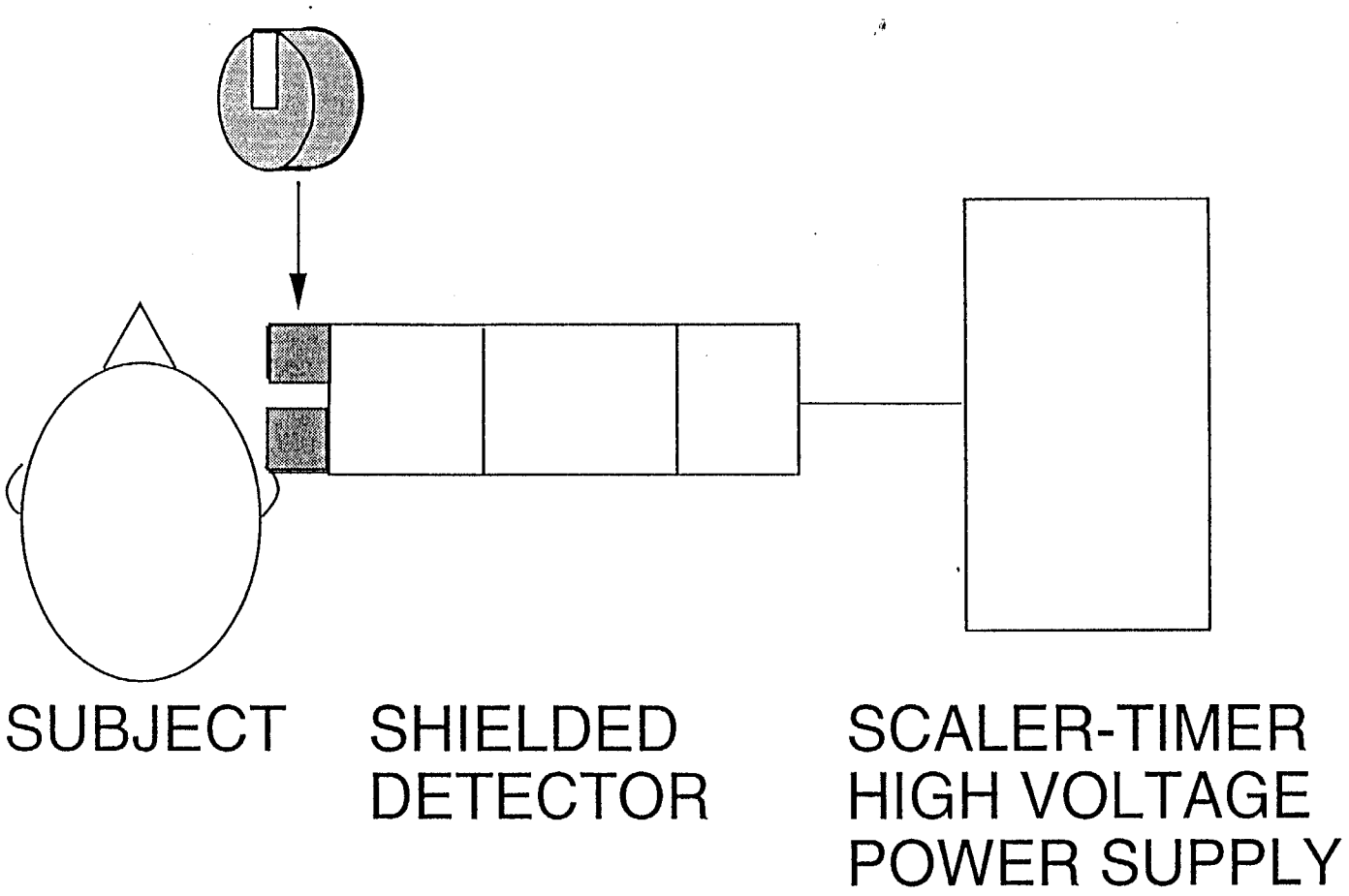
SUBJECT
SHIELDED
DETECTOR
SCALER-TIMER
HIGH VOLTAGE
POWER SUPPLY

Figure 5:

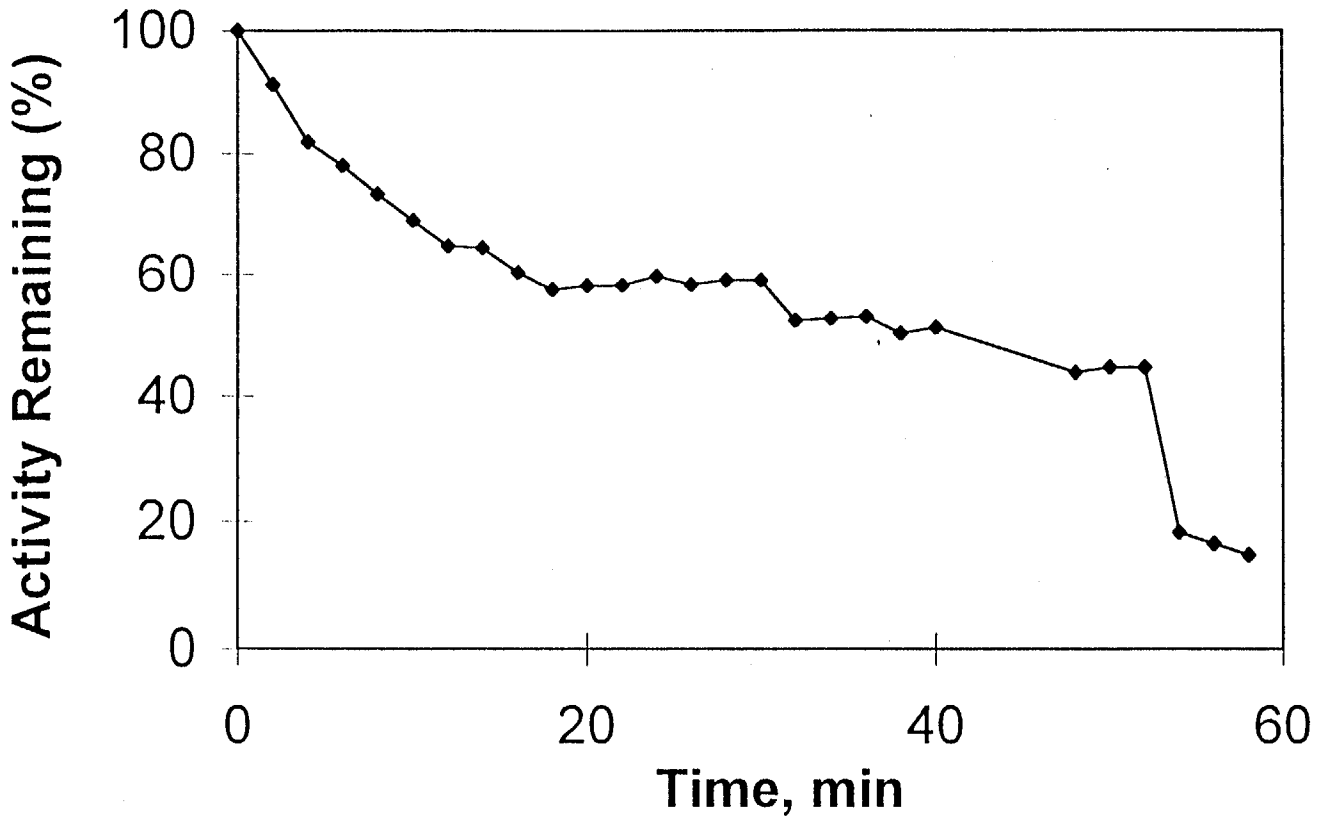

Figure 6

AN EXPERIMENTAL METHOD FOR MEASURING DEPOSITION EFFICIENCY OF ULTRAFINE AEROSOLS IN HUMAN ORAL AIRWAY*

Kuo-Hsi Cheng[a], Yung-Sung Cheng[b], Hsu-Chi Yeh[b], and David L. Swift[a]

[a]Department of Environmental Health Sciences,
The Johns Hopkins School of Hygiene and Public Health,
Baltimore, MD 21205;
[b]Inhalation Toxicology Research Institute, P.O. Box 5890,
Albuquerque, NM 87185

Corresponding Author: David L. Swift, Ph.D.
Room 6010
Department of Environmental Health Sciences
Johns Hopkins University
School of Hygiene and Public Health
615 North Wolfe Street
Baltimore, MD 21205

Abbreviated Title: A Method for Measuring Oral Deposition

---

*Research was carried out at the Inhalation Toxicology Research Institute (ITRI), and supported by the Office of Health and Environmental Research, U.S. Department of Energy under contract Numbers DE-FG02-88ER60655 at Johns Hopkins University and DE-AC04-76EV01013 at ITRI.

ABSTRACT

Although mouth breathing is common while exercising, speaking, and singing, information on particles deposited in the oral airway during these activities is rather limited. In the present study, an experimental technique was proposed to measure the oral deposition of inhaled particles by using an external pump to draw test aerosols through the nose and mouth (passive method) and an oral extension tube. A replicate human upper airway cast was challenged with monodisperse particles ranging in size from 3.6 to 150.0 nm at constant flow rates of 7.5 to 30 L/min. For the inhalation study, test aerosols were drawn into the nasal cavity and directed either through the laryngeal-tracheal (L-T) section or the oral passage with/without the oral extension tube inserted up to uvula of the cast. These flow patterns were reversed for the exhalation study. Deposition efficiencies of inhaled particles in the main oral cavity were found approximately equal to those in the L-T section for both inhalation and exhalation. The results of analysis of variance showed that empirical measurements of particle deposition via the mouth-trachea path agreed well with the calculated oral deposition efficiencies based on the experimental data of aerosol intake via the nose-mouth path with/without insertion of the oral extension tube. The similarities between the empirical and calculated oral

deposition suggest that the passive method combined with an oral extension tube is appropriate for determining deposition efficiencies of ultrafine particles in the oral airway. This noninvasive method has potential application for determining the oral deposition of micrometer-sized particles, which are often encountered in occupational environments.

Deposition of particles in the human extrathoracic airways, including the nose, mouth, pharynx, and larynx, is an important protective mechanism for the respiratory tract. It has been well documented that the nasal passage effectively warms and humidifies inspired air, removes aerosol particles and gases from inspired air, and detects odorants contained in inspired air.[1,2] At a sufficiently high rate of breathing, a normal nose breather will augment nasal flow by breathing partly through the low-resistance oral passage.[3] Humans breathe through the mouth while speaking and singing[4] and breathe entirely through the oral route if the nose is obstructed due to allergy or infection. Although mouth breathing is common, the significant role of the oral airway in respiratory defense by filtering particles has not been systematically examined.[5] When air is inspired through the mouth, the oral passage becomes the first line of protection for the lungs. The switch of breathing route from the nasal to oral passage is particularly important in assessing occupational exposure to toxic particles, because workers often need elevated respiratory ventilation and constant verbal communication for performing their tasks. Besides exposure to occupationally derived pollutants, many workers who smoke inhale cigarette particles through their mouth. A 50-state prospective study by the American Cancer Society reported that the relative risk of death among male smokers over 35 years of age was 27.48 for oral

cavity cancer and 10.48 for laryngeal cancer, compared with nonsmokers.[6]

For aerosol deposition in the nasal airway, coarse particles in a size range from 0.5 to 10 μm [7-12] and ultrafine particles ranging from 0.0005 to 0.2 μm in diameter [13-18] have been studied extensively. However, relatively few studies have measured the oral deposition. Lippmann,[8] Foord et al.,[19] and Chan and Lippmann[20] have measured *in vivo* the oral deposition of micrometer-sized particles in a study that aimed to determine lung deposition. Gamma-labeled monodisperse aerosols were inhaled normally into the lungs through a mouthpiece, and the fraction of particles deposited in the mouth was determined by external radioactive counting. Unfortunately, spatial resolution and tissue attenuation severely limited the accuracy of radioactive counting for the amount of deposited particles. In the study by Bowes and Swift,[5] subjects inhaled fluorescent tracer particles during natural oronasal breathing and gargled to collect the fraction of particles deposited in the oral cavity. This study suggested that the filtration efficiency of the oral passage was sensitive to the configuration of the mouth opening. A problem arose when determining how far back in the posterior oral cavity could particles be recovered by the rinsing solutions.

Exposure to radon progeny has been linked to an increased occurrence of lung cancer in underground miners,[21] and has been experimentally shown

to cause lung cancer and nasal carcinoma in laboratory animals.[22] The size range of radon progeny in the mining and home environments corresponds to ultrafine particles. Estimates of oral filtration efficiency of ultrafine aerosols have been developed using human replicate upper airway casts.[14,15,23] The results of these studies showed that oral deposition increased with decreasing particle size and flow rate, and that the oral airway was a less efficient collector of ultrafine particles compared to the nasal airway at any combination of flow rate and particle size. The less efficient filtration of the oral airway implies that the fraction of inhaled particles penetrating into the tracheobronchial and pulmonary regions may increase during mouth breathing. However, no information is available regarding *in vivo* measurements of ultrafine particles deposited in the oral airway.

A systematic study of ultrafine aerosol deposition in the nasal and oral airways of human subjects using the passive breathing method is underway in our laboratories. The present study was undertaken to examine whether oral deposition could be reasonably estimated by inserting an extension tube in the mouth. Using a human replicate upper airway cast, the oral deposition efficiencies calculated from experimental data of four breathing maneuvers were compared to those measured empirically in the oral airway. This noninvasive method is particularly useful for measuring *in vivo* the oral

deposition of nonradioactive aerosols.

EXPERIMENTAL METHODS

Replicate Airway Model

A replicate human upper airway cast (the second model made from Adult-Nasal-Oral-Tracheal head airway casts; denoted ANOT2) containing a nasal cavity, an oral cavity, and a laryngeal-tracheal (L-T) section was used to measure deposition efficiencies of ultrafine aerosols in the oral airway. Model ANOT2 was constructed from a postmortem nasal cast and an *in vivo* oral cast. The anterior oral cavity which was cast from dental impression of a living male adult represents a relatively opened mouth. The nasal passage conformed to the nasal dimensions of models A and B described by Swift et al.[17] The oropharynx, larynx, and upper trachea sections were supplied by Dr. James Bosma, while at the National Institute of Health. Another clear polyester resin block with an identical oral cavity and L-T airway was mechanically sliced at 3-mm intervals. The periphery of the airway contour for each 3-mm section was traced and digitized by a GRAF/PEN sonic digitizer (SAC, Southport, Connecticut). Based on these digitized data, the cross-sectional areas and perimeters in the coronal plane at a resolution of 3 mm for a distance from the lips to the oropharynx were calculated (Figure 1).

Experimental System

Figure 2 shows the experimental system used to expose the cast. It consisted of the components for aerosol generation, particle size classification, concentration measurement, and aerosol sampling. Polydisperse silver particles produced by a furnace or polystyrene latex (PSL) particles aerosolized by a nebulizer were passed into an electrostatic classifier (UCPC; TSI Model 3071, St. Paul, MN) to obtain a fraction of monodisperse particles. These monodisperse aerosols were then brought to Boltzmann equilibrium charge distribution in a ^{85}Kr discharger and diluted with filtered air to obtain any desired flow rates. Upstream and downstream concentrations were measured by an ultrafine condensation particle counter (TSI Model 3025, St. Paul, MN). A model 386/33 personal computer, equipped with Labtech Notebook version 6.1.2. software (Laboratory Technologies Corp., San Francisco, CA) and the Strawberry Tree ACPC-12-16 data acquisition interface card (Strawberry Tree Incorporated, Sunnyvale, CA) was used to control the system operation and record the experimental data.

The condensation aerosol generator was similar to the one described by Tu and Kanapilly[24] and Scheibel and Porstendörfer.[25] The operating principle was based on the theory that very fine particles could be formed by the process of homogeneous nucleation from a supersaturated vapor. The

aerosol generator contained a carrier tube and a glass boat in which the aerosol material was placed; both were electrically heated by a furnace (Thermcraft, Winston-Salem, NC) to between 850 to 1000°C. A nitrogen gas stream regulated at constant flow rate of 2.5 L/min was introduced to carry the vaporized aerosol material into a cooler glass chamber. The aerosol transport line was disconnected from the furnace, and a Retec X-70 nebulizer was connected to the silica gel drier when generating PSL particles (Duke Scientific Corp., Palo Alto, CA). A TSI Model 3071 electrostatic classifier consisting of a bipolar diffusion charger and a differential mobility analyzer was used to obtain monodisperse silver and PSL particles of known size. The physical properties of electrical mobility classifier, including size distributions, mobility distributions, and the ratio of singly to doubly charged fractions have been reported by Cheng and Denee.[26] Particle sizes were also calibrated using a screen diffusion battery described by Cheng et al.[13]

Because the inlet and outlet aerosol concentrations were measured by a single TSI 3025 UCPC, the absolute value of UCPC detection efficiency was not a concern; only the relative ratio of concentrations was needed in this study. Aerosol concentrations were adjusted to < 1500 particles/cm^3 so that the UCPC could be operated in the single-particle real-time counting mode. Upstream and downstream aerosol concentrations of the airway model were

sampled through the control of a three-way solenoid valve (Fluorocarbon, Anaheim, CA).

Exposure Procedures

Silver wools were used to produce particles < 20 nm in diameter. To generate particles > 100 nm, PSL particles in aqueous suspension were aerosolized. Before the experiments, the inner surface of the model was coated with an anti-static liquid (Zero Charge Anti-stat, Tech Spray Inc., Amarillo, TX) to reduce the electrostatic effect on particle deposition. Six particle sizes (3.6, 5, 8, 20, 100, and 150 nm) were tested at four constant flow rates (7.5, 10, 20, and 30 L/min).

The experimental protocol consisted of three phases. Phase I was an indirect method of calculating oral deposition efficiencies based on experimental measurements of particle deposition in six breathing paths. These included nose-in-mouth-out ($N_{in}M_{out}$), mouth-in-nose-out ($M_{in}N_{out}$), nose-in-trachea-out ($N_{in}T_{out}$), trachea-in-nose-out ($T_{in}N_{out}$), nose-in-mouth-out with oral extension tube (N_{in}), and mouth-in-nose-out with oral extension tube (N_{out}). The extension tube inserted up to the uvula was intended to bypass the majority of the oral cavity. After correction for particle losses in the connecting tubes, the measurements made in the breathing paths with the oral

extension tube could represent the Inspiratory and Expiratory Nasal-Pharyngeal (INP and ENP, respectively) deposition. Test aerosols were passively drawn into the nasal airway and directed either through the L-T airway or the oral passage for the inhalation study; flow patterns were reversed for the exhalation study. Deposition efficiencies were measured four times for each combination of particle size and flow rate.

If the respiratory tract is considered as a series of many particle filters, the probability of a particle entering the n^{th} filter is equal to the product of the penetration efficiencies of previous n-1 filters. Thus, the Inspiratory Oral Cavity (IOC) and Expiratory Oral Cavity (EOC) deposition efficiencies could be calculated by:

$$IOC\ Deposition = 1 - \frac{1 - \eta(M_{in}N_{out})}{1 - \eta(N_{out})} \quad (1)$$

$$EOC\ Deposition = 1 - \frac{1 - \eta(N_{in}M_{out})}{1 - \eta(N_{in})} \quad (2)$$

where $\eta(N_{in}M_{out})$ and $\eta(M_{in}N_{out})$ are the deposition efficiencies for the nose-mouth path during inhalation and exhalation, and $\eta(N_{in})$ and $\eta(N_{out})$ are the deposition efficiencies for the nose-mouth path with the oral extension tube during inhalation and exhalation. Similar relationships could be established for

calculating the Inspiratory L-T (ILT) and Expiratory L-T (ELT) deposition efficiencies:

$$ILT\ Deposition = 1 - \frac{1 - \eta(T_{in}N_{out})}{1 - \eta(N_{out})} \quad (3)$$

$$ELT\ Deposition = 1 - \frac{1 - \eta(N_{in}T_{out})}{1 - \eta(N_{in})} \quad (4)$$

where $\eta(N_{in}T_{out})$ and $\eta(T_{in}N_{out})$ are the deposition efficiencies for the nose-trachea path during inhalation and exhalation. Given the data of IOC, EOC, ILT, and ELT deposition, the Inspiratory Oral-Laryngeal-Tracheal (IOLT) and Expiratory Oral-Laryngeal-Tracheal (EOLT) deposition efficiencies could be calculated by

$$IOLT\ Deposition = 1 - [1 - IOC\ Deposition][1 - ILT\ Deposition] \quad (5)$$

$$EOLT\ Deposition = 1 - [1 - ELT\ Deposition][1 - EOC\ Deposition] \quad (6)$$

Phase II was a direct measurement of ultrafine aerosol deposition in the oral airway of model ANOT2. The aerosol was drawn into the mouth and out of the trachea for inhalation; the flow pattern was reversed for exhalation. Each combination of particle size and flow rate was measured four times. The net IOLT and EOLT depositions were also corrected for the losses inherent to the transport lines.

The data obtained from Phases I and II were compared using statistical analysis. Three sets of statistical analysis were performed in phase III, including a comparison of (1) calculated IOLT and EOLT depositions obtained from phase I, (2) empirical IOLT and EOLT depositions obtained from phase II, and (3) calculated versus empirical IOLT and EOLT deposition. Because the same particle sizes and flow rates were used for each breathing path, the experimental data could be stratified accordingly with a total strata of 24 to compare two corresponding treatments.[27] The pooled mean difference of deposition efficiencies between two paths was a weighted average of these 24 pairs of differences between two means in each stratum. The weighting factor (W_i) was related to the number of samples for the first path (n_{1i}) and the second path (n_{2i}) in each stratum (i) as $W_i = n_{1i}n_{2i}/(n_{1i}+n_{2i})$ under the assumption that the variance of the response variable (deposition efficiency) was the same for both paths and in all strata. The test statistic for the mean difference was calculated using one-way analysis of variance (ANOVA).

RESULTS

Figure 1 shows the cross-sectional areas and perimeters as a function of the oral distance from the lips (defined as the origin) to the posterior oral cavity (72 mm) at 3-mm intervals. The maximum cross-sectional area occurred

near the oropharynx, while the perimeter reached a broaden peak at the middle oral cavity. The surface area and average cross-sectional area for the entire 72-mm oral distance were calculated to be 101.95 and 6.90 cm^2, respectively. Table I shows the distribution of regional deposition in the oral cavity, nasal-pharyngeal region, and L-T section. Deposition efficiencies in the oral cavity were observed approximately equal to those in the L-T section during both inhalation and exhalation for the range of particle sizes and flow rates studied. For 3.6-nm particles, the deposition efficiencies were found to be about 18% in the nasal-pharyngeal region, 6% in the oral cavity, and 6% in the L-T section at a flow rate of 30 L/min.

Tables II and III present the results of calculated and empirical IOLT and EOLT deposition efficiencies. The general trend of increasing particle deposition with decreasing particle diameter and flow rate was consistent with previous findings based on other oral and nasal casts.[13-18] Particle deposition decreased monotonically as particle diameter increased and reached a minimum efficiency of less than 3% at 150 nm. The effect of flow rate on the deposition of 100 and 150 nm particles was not clear because the experimental errors were significant relative to the low deposition efficiencies of these particles. Comparisons of empirical versus calculated and inspiratory versus expiratory oral deposition are summarized in Table IV. The ANOVA

indicated that empirical measurements of particle deposition via the mouth-trachea path were not significantly different from the deposition efficiencies calculated from the experimental data via the nose-mouth path with/without insertion of an oral extension tube for both inhalation ($F_{1,144}$= 1.074; p=0.302) and exhalation ($F_{1,144}$=1.015; p=0.315). Particle depositions during inhalation and exhalation were also compared for the calculated and empirical methods. Results showed that oral deposition of ultrafine aerosols was slightly higher during inhalation compared to exhalation for both calculated and empirical data. However, the magnitude of difference was small and not significant at the 95% confidence level.

DISCUSSION

In the present study, we have shown that oral deposition of ultrafine aerosols can be reasonably estimated by inserting an extension tube into the mouth. The proposed experimental protocol consists of four breathing maneuvers: breathing in through the nose and out through the mouth (nose-in-mouth-out), breathing in through the mouth and out through the nose (mouth-in-nose-out), nose-in-mouth-out with an oral extension tube, and mouth-in-nose-out with an oral extension tube. The oral extension tube is designed to bypass the oral cavity.

Because the oral cavity of model ANOT2 was cast using a dental impression method which required a supporting mouthpiece to separate the teeth and enlarge the airway, the widely opened passage might be equivalent to the mouth opening during moderate or heavy exercise. As mentioned above, occupational tasks often demand higher activity levels. A widely opened oral passage represents the airway configuration of the mouth through which airborne particles and gases are inhaled under typical conditions in the workplace. Although the two lower flow rates (7.5 and 10 L/min) did not seem practical for such a wide mouth opening, they were used to study the effect of respiratory ventilation on particle deposition. Normal nose breathers were found to switch from 100% nasal breathing to about 43% mouth breathing at a respiratory flow rate of 35 L/min.[28,29] Oral ventilation increased to 60% as the total respiratory flow rate increased to 90 L/min.[29] This implies that the 20 and 30 L/min used in the present study can represent the proportion of the total airflow inhaled through the mouth under moderate or heavy exercise of approximately 45 and 60 L/min.

With insertion of an oral extension tube up to the uvula, a regional distribution of particle deposition in the nasal-pharyngeal region, oral cavity, and L-T section could be determined. The insignificant difference in particle deposition found in the oral cavity and L-T section leads to an interesting

discussion about why an apparent difference in the airway structure results in a similar particle filtration efficiency. Because turbulent diffusion is the major mechanism responsible for the deposition of ultrafine particles in the respiratory tract, the likelihood of particles deposited onto the airway walls by diffusion increases with longer residence time and more turbulent flow. The smaller cross-sectional area and more complex airway shape of the L-T section will increase the probability of mass transport in the direction toward the airway walls by turbulent diffusion. On the other hand, the larger volume of the oral cavity will result in a longer residence time of inhaled particles. Thus, the balance between flow turbulence and residence time probably accounts for the similar particle deposition found in the oral cavity and the L-T section.

The insignificant difference between the calculated and empirical IOLT or EOLT deposition suggests that the use of the passive method with an oral extension tube is appropriate for determining the oral deposition of ultrafine aerosols. Several studies have measured the oral deposition of micrometer-sized particles in human subjects.[5,20,30] However, little *in vivo* information is available regarding the deposition of ultrafine aerosols in the oral airway. Various occupationally derived gases and particles have been identified as potential agents for developing thoracic diseases, such as asthma,

pneumoconiosis, bronchitis, and lung cancers.[1] When the nasal route is bypassed, the oral airway is the first protection for the lung. To establish appropriate exposure-dose relationships for the lung, it is important to understand the deposition and absorption of inhaled particles and gases in the oral airway. In addition to direct application in radon progeny dosimetry, the oral deposition data of ultrafine particles obtained from the present study can be extrapolated to diffusing gases and vapors if the air-mucosa interface of a gas or vapor can be specified.

In conclusion, the present study not only presents a methodology appropriate for measuring *in vivo* deposition of ultrafine aerosols in the oral airway, but suggests a noninvasive technique potentially applicable in determining the oral deposition of micrometer-sized particles. As mouth breathing is common, information about the extrathoracic filtration would not be complete without extensive understanding of the aerosol deposition in the oral passage. A better exposure-dose assessment for the extrathoracic airways is essential in establishing more appropriate dose-response relationships for the intrathoracic airways.

ACKNOWLEDGEMENT

The authors thank Rick D. Brodbeck and Thomas D. Holmes for their technical assistance in establishing the aerosol exposure system, and P. L. Bradley for her editorial help at ITRI.

REFERENCES

1. **Bouhuys, A.:** *Breathing - Physiological, Environmental, and Lung Disease.* New York, NY: Grune & Stratton, 1974. pp. 25-27, 342-376.

2. **Lang, J.:** *Clinical Anatomy of the Nose, Nasal Cavity, and Paranasal Sinuses.* (Translated by Stell, P. M.), New York, NY: Thieme Medical Publishers, 1989. p. 119.

3. **National Research Council (NRC):** *Panel on Dosimetric Assumptions Affecting the Application of Radon Risk Estimates Comparative Dosimetry of Radon in Mines and Homes - Companion to BEIR IV.* Washington, D.C.: National Academy Press, 1991. pp. 152, 219-222.

4. **Camner, P. and B. Bakke:** Nose or Mouth Breathing? *Environ. Res.* 21:394-398 (1980).

5. **Bowes III, S. M. and D. L. Swift:** Deposition of Inhaled Particles in the Oral Airway During Oronasal Breathing. *Aerosol Sci. & Technol.*

11:157-167 (1989).

6. **Department of Health and Human Services (DHHS):** *Smoking, Tobacco, and Cancer Program, 1985-1989 Status Report.* Washington D.C.: Government Printing Office, 1990. DHHS (NIH) Publication No. 90-3107.

7. **Pattle, R. E.:** The Retention of Gases and Particles in the Human Nose. In *Inhaled Particles and Vapors.* C. N. Davis, ed. Great Britain: Pergamon Press, 1961. pp. 302-309.

8. **Lippmann, M:** Deposition and Clearance of Inhaled Particles in the Human Nose. *Ann. Otol. Rhinol. Laryngol.* 79: 519-528 (1970).

9. **Hounam, R. F., A. Black, and M. Walsh:** The Deposition of Aerosol Particles in the Nasopharyngeal Region of the Human Respiratory Tract. *J. Aerosol Sci.* 2:47-61 (1971).

10. **Giacomelli-Maltoni, G., C. Melandri, V. Prodi, and G. Tarroni:** Deposition Efficiency of Monodisperse Particles in Human Respiratory Tract. *Am. Ind. Hyg. Assoc. J.* 33:603-610 (1972).

11. **Fry, F. A. and A. Black:** Regional Deposition and Clearance of Particles in the Human Nose. *J. Aerosol Sci.* 4: 113-124 (1973).

12. **Heyder, J. and G. Rudolf:** Deposition of Aerosol Particles in the Human Nose. In *Inhaled Particles IV.* W. H. Walton, ed. Great

Britain: Pergamon Press, 1977. pp.107-126.

13. **Cheng, Y. S., Y. Yamada, H. C. Yeh, and D. L. Swift:** Diffusional Deposition of Ultrafine Aerosols in A Human Nasal Cast. *J. Aerosol Sci.* 19(6):741-751 (1988).

14. **Cheng, Y. S., H. C. Yeh, and D. L. Swift:** Aerosol Deposition in Human Nasal Airway for Particles 1 nm to 20 μm: A Model Study. In *Radiation Protection Dosimetry.* R. A. Guilmette and B. B. Boecker, ed. Great Britain: Nuclear Technology Publishing. Vol 38, No. 1/3, 1991. pp. 41-47.

15. **Cheng, Y. S., Y. F. Su, H. C. Yeh, and D. L. Swift:** Deposition of Thoron Progeny in Human Head Airways. *Aerosol Sci. & Technol.* 18:359-375 (1993).

16. **Strong, J. C. and D. L. Swift:** Deposition of Unattached Radon Daughters in Models and Human Nasal Airways. In *Indoor Radon and Lung Cancer: Realty or Myth?: Twenty-ninth Hanford Symposium on Health and the Environment.* F. T. Cross, ed. Richland, WA: Battelle Press, 1992. p. 227.

17. **Swift, D. L., N. Montassier, P. K. Hopke, K. Karpen-Hayes, Y-S. Cheng, Y-F. Su, H-C. Yeh, and J. C. Strong:** Inspiratory Deposition of Ultrafine Particles in Human Nasal Replicate Casts. *J. Aerosol Sci.*

23(1):65-72 (1992).

18. **Swift, D. L., Y. S. Cheng, Y. F. Su, and H. C. Yeh:** Ultrafine Aerosol Deposition in the Human Nasal and Oral Passages. In *Inhaled Particles VII.* J. Dodgson and R. I. McCallum, ed. Great Britain: Pergamon, 1994. pp. 77-81.

19. **Foord, N., A. Black, and M. Walsh:** Regional Deposition of 2.5-7.5 Micrometer Diameter Inhaled Particles in Healthy Male Nonsmokers. *J. Aerosol Sci.* 9:343-357 (1978).

20. **Chan, T. L. and M. Lippmann:** Experimental Measurements and Empirical Modeling of the Regional Deposition of Inhaled Particles in Humans. *Am. Ind. Hyg. Assoc. J.* 41:399-408 (1980).

21. **National Research Council (NRC):** *Health Risk of Radon and Other Internally Deposited Alpha-Emitters.* Committee on the Biological Effects of Ionizing Radiations, BEIR IV, Washington, D.C.: National Academy Press, 1988.

22. **Cross, F. T.:** Radiation Inhalation Studies in Animals. *Radiat. Prot. Dosim.* 24:463-466 (1988).

23. **Gradon, L. and C. P. Yu:** Diffusional Particle Deposition in the Human Nose and Mouth. *Aerosol Sci. & Technol.* 11:213-220 (1989).

24. **Tu, K. W. and G. M. Kanapilly:** Generation and Characterization of

Submicron Ammonium Sulfate and Ammonium Hydrogen Sulfate Aerosols. *Aerosol Atmos. Environ.* 12:1623-1629 (1978)

25. **Scheibel, H. G. and J. Porstendörfer:** Generation of Monodisperse Ag- and NaCl- Aerosols with Particle Diameters Between 2 and 300 nm. *J. Aerosol Sci.* 14(2):113-126 (1983).

26. **Cheng, Y. S., and P. B. Denee:** Physical Properties of Electrical Mobility Classified Aerosols. *J. Coll. and Interface Sci.* 80(1):284-293 (1981).

27. **Fleiss, J. L.:** *The Design and Analysis of Clinical Experiments.* New York: John Wiley & Sons, 1986. pp. 149-181.

28. **Niinimaa, W., P. Cole, S. Mintz, and R. J. Sherphard:** The Switching Point from Nasal to Oronasal Breathing. *Respir. Physiol.* 42:61-71 (1980).

29. **Niinimaa, W., P. Cole, S. Mintz, and R. J. Sherphard:** Oronasal Distribution of Respiratory Flow. *Respir. Physiol.* 43:69-75 (1981).

30. **Stahlhofen, W., J. Gebhart, and J. Heyder:** Experimental Determination of the Regional Deposition of Aerosol Particles in the Human Respiratory Tract. *Am. Ind. Hyg. Assoc. J.* 41:385-398 (1980).

TABLE I. Aerosol Deposition in the Nasal-Pharyngeal (N-P) Region, the Oral Cavity, and the Laryngeal-Tracheal(L-T) Section of Model ANOT2

Particle Size (nm)	Flow Rate (L/min)	N-P Region (%)		Oral Cavity (%)		L-T Section(%)	
		Inhalation	Exhalation	Inhalation	Exhalation	Inhalation	Exhalation
3.6	7.5	20.1 ± 1.6	20.5 ± 1.5	7.9 ± 1.9	7.5 ± 1.7	8.9 ± 3.2	7.7 ± 1.6
5	7.5	12.5 ± 1.7	14.8 ± 1.5	6.4 ± 1.3	8.5 ± 1.4	4.7 ± 1.7	2.5 ± 1.5
8	7.5	7.8 ± 2.0	9.1 ± 2.0	4.6 ± 1.7	5.6 ± 1.8	5.3 ± 2.5	3.5 ± 1.8
20	7.5	5.2 ± 2.5	5.9 ± 2.7	2.2 ± 2.9	3.1 ± 2.3	3.7 ± 2.8	2.5 ± 2.3
100	7.5	1.8 ± 1.3	2.3 ± 1.4	0.2 ± 1.2	0.4 ± 1.9	0.1 ± 0.9	0.1 ± 1.2
150	7.5	2.8 ± 1.2	2.9 ± 1.1	0.2 ± 1.5	0.3 ± 1.0	0.1 ± 1.2	0.1 ± 0.7
3.6	10	22.3 ± 2.4	21.2 ± 2.2	7.4 ± 2.1	0.5 ± 3.0	6.7 ± 2.6	7.5 ± 2.8
5	10	14.2 ± 2.2	14.3 ± 2.0	4.6 ± 1.4	4.0 ± 2.0	3.4 ± 2.5	3.3 ± 2.1
8	10	7.7 ± 2.2	8.1 ± 2.4	3.8 ± 3.3	4.7 ± 1.7	5.5 ± 2.4	3.8 ± 2.6
20	10	5.3 ± 1.9	4.1 ± 2.0	2.3 ± 2.5	1.7 ± 1.5	4.2 ± 2.4	5.2 ± 1.9
100	10	1.6 ± 1.7	2.7 ± 1.9	0.2 ± 2.1	0.3 ± 1.7	0.1 ± 1.0	0.1 ± 1.8
150	10	0.2 ± 1.6	1.3 ± 1.9	0.1 ± 2.1	0.8 ± 1.8	0.1 ± 2.0	0.1 ± 1.9
3.6	20	20.1 ± 2.6	20.7 ± 2.2	8.4 ± 4.1	5.1 ± 2.9	4.6 ± 3.0	5.0 ± 3.2
5	20	16.2 ± 1.5	15.4 ± 1.5	5.9 ± 2.0	4.2 ± 1.5	1.4 ± 1.9	1.8 ± 1.4
8	20	6.7 ± 1.6	5.9 ± 1.9	7.0 ± 3.4	3.2 ± 3.0	4.6 ± 2.6	5.8 ± 2.6
20	20	3.2 ± 2.1	5.3 ± 2.4	2.2 ± 2.1	3.3 ± 2.7	3.7 ± 2.5	1.9 ± 2.0
100	20	0.1 ± 1.6	0.7 ± 0.8	0.9 ± 0.9	1.4 ± 1.7	0.9 ± 1.7	0.4 ± 0.6
150	20	0.1 ± 2.3	0.1 ± 1.2	0.4 ± 1.3	0.5 ± 2.3	0.3 ± 2.5	0.5 ± 1.0
3.6	30	17.6 ± 3.1	18.8 ± 3.0	6.1 ± 3.6	6.3 ± 3.9	5.8 ± 3.6	5.6 ± 4.5
5	30	11.5 ± 1.8	11.7 ± 2.0	4.0 ± 2.4	3.6 ± 2.2	2.8 ± 2.8	4.4 ± 2.9
8	30	7.8 ± 1.0	7.3 ± 1.1	3.4 ± 0.9	2.8 ± 1.5	2.0 ± 1.1	4.4 ± 3.1
20	30	3.8 ± 1.5	4.1 ± 1.9	1.9 ± 2.1	1.5 ± 1.6	1.7 ± 2.0	1.6 ± 3.4
100	30	0.9 ± 2.1	1.2 ± 1.4	0.4 ± 2.3	0.2 ± 2.8	0.2 ± 2.6	1.1 ± 1.8
150	30	1.8 ± 2.3	2.6 ± 1.9	0.1 ± 2.0	0.7 ± 1.5	2.0 ± 1.9	0.3 ± 1.0

*Abbreviations in the table are:
N-P: Nasal-Pharyngeal; L-T: Laryngeal-Tracheal

TABLE II. Calculated Inspiratory Oral-Laryngeal-Tracheal (IOLT) and Expiratory Oral-Laryngeal-Tracheal (EOLT) Depositions in Model ANOT2

Number of Stratum	Number of Samples	Particle Size (nm)	Flow Rate (L/min)	Calculated Efficiency (%)			
				IOLT		EOLT	
				Mean	S.D.	Mean	S.D.
1	4	3.6	7.5	16.0	4.2	14.7	2.5
2	4	5	7.5	10.8	2.2	10.8	2.3
3	4	8	7.5	9.6	3.2	8.9	2.7
4	4	20	7.5	5.9	4.2	6.5	3.8
5	4	100	7.5	0.3	1.5	0.5	2.3
6	4	150	7.5	0.2	1.9	0.3	1.2
7	4	3.6	10	13.6	3.6	13.5	4.3
8	4	5	10	7.8	2.9	7.1	3.1
9	4	8	10	9.1	4.4	8.4	3.3
10	4	20	10	6.4	3.6	6.8	2.4
11	4	100	10	0.3	2.4	0.4	2.5
12	4	150	10	0.1	2.9	0.3	2.7
13	4	3.6	20	12.6	5.2	10.1	4.5
14	4	5	20	7.3	2.7	5.9	2.1
15	4	8	20	11.2	4.4	8.8	4.0
16	4	20	20	5.8	3.4	5.2	3.5
17	4	100	20	1.8	1.9	1.8	1.8
18	4	150	20	0.6	2.8	1.0	2.5
19	4	3.6	30	11.6	5.4	11.6	6.4
20	4	5	30	6.7	3.8	7.9	3.8
21	4	8	30	5.3	1.5	7.1	3.5
22	4	20	30	3.6	3.2	3.1	3.8
23	4	100	30	0.6	3.4	1.3	3.3
24	4	150	30	1.6	2.8	0.9	1.9

*Abbreviations in the table are:
IOLT: Inspiratory Oral-Laryngeal-Tracheal; EOLT: Expiratory Oral-Laryngeal-Tracheal; S.D.: Standard Deviation.

TABLE III. Empirical Inspiratory Oral-Laryngeal-Tracheal (IOLT) and Expiratory Oral-Laryngeal-Tracheal (EOLT) Depositions in Model ANOT2

Number of Stratum	Number of Samples	Particle Size (nm)	Flow Rate (L/min)	Empirical Efficiency (%)			
				IOLT		EOLT	
				Mean	S.D.	Mean	S.D.
1	4	3.6	7.5	16.8	1.6	14.6	3.0
2	4	5	7.5	10.1	1.7	9.5	1.9
3	4	8	7.5	10.9	1.8	8.9	1.9
4	4	20	7.5	2.3	2.8	3.5	1.8
5	4	100	7.5	1.3	1.5	1.4	1.1
6	4	150	7.5	3.6	1.2	2.0	1.1
7	4	3.6	10	17.9	3.0	18.1	3.7
8	4	5	10	8.1	2.1	7.2	2.1
9	4	8	10	9.9	2.7	8.8	2.3
10	4	20	10	1.4	2.0	3.0	2.0
11	4	100	10	1.0	1.7	1.0	2.0
12	4	150	10	1.1	1.9	0.5	1.1
13	4	3.6	20	16.6	2.8	16.9	2.1
14	4	5	20	12.2	1.1	13.0	2.3
15	4	8	20	7.7	2.5	7.5	2.2
16	4	20	20	0.5	2.9	0.7	2.2
17	4	100	20	0.1	1.1	0.1	1.3
18	4	150	20	0.2	1.2	0.3	1.3
19	4	3.6	30	16.4	1.6	15.5	2.3
20	4	5	30	8.3	1.5	7.6	1.5
21	4	8	30	8.2	1.6	6.8	1.8
22	4	20	30	2.0	3.0	4.1	1.0
23	4	100	30	0.4	0.8	0.8	2.0
24	4	150	30	2.2	2.7	0.9	2.4

*Abbreviations in the table are:
IOLT: Inspiratory Oral-Laryngeal-Tracheal; EOLT: Expiratory Oral-Laryngeal-Tracheal; S.D.: Standard Deviation.

TABLE IV. *Comparisons of Empirical and Calculated Inspiratory Oral-Laryngeal-Tracheal (IOLT) and Expiratory Oral-Laryngeal-Tracheal (EOLT) Deposition Efficiencies*

CATEGORY	POOLED MEAN COMPARISON	POOLED MEAN DIFFERENCE (%)	$F_{1,144}$ VALUE	p VALUE
IOLT Deposition	$IOLT_{emp} > IOLT_{cal}$	0.42	1.074	0.302
EOLT Deposition	$EOLT_{emp} > EOLT_{cal}$	0.40	1.015	0.315
Empirical Deposition	$IOLT_{emp} > EOLT_{emp}$	0.28	0.883	0.349
Calculated Deposition	$IOLT_{cal} > EOLT_{cal}$	0.26	0.281	0.597

*Abbreviations in the table are:

$IOLT_{cal}$: Calculated Inspiratory Oral-Laryngeal-Tracheal deposition
$EOLT_{cal}$: Calculated Expiratory Oral-Laryngeal-Tracheal deposition
$IOLT_{emp}$: Empirical Inspiratory Oral-Laryngeal-Tracheal deposition
$EOLT_{emp}$: Empirical Expiratory Oral-Laryngeal-Tracheal deposition

FIGURE CAPTION LISTING

FIGURE 1. Cross-sectional areas and perimeters for the oral cavity of model ANOT2

FIGURE 2. Experimental setup for the cast exposure system

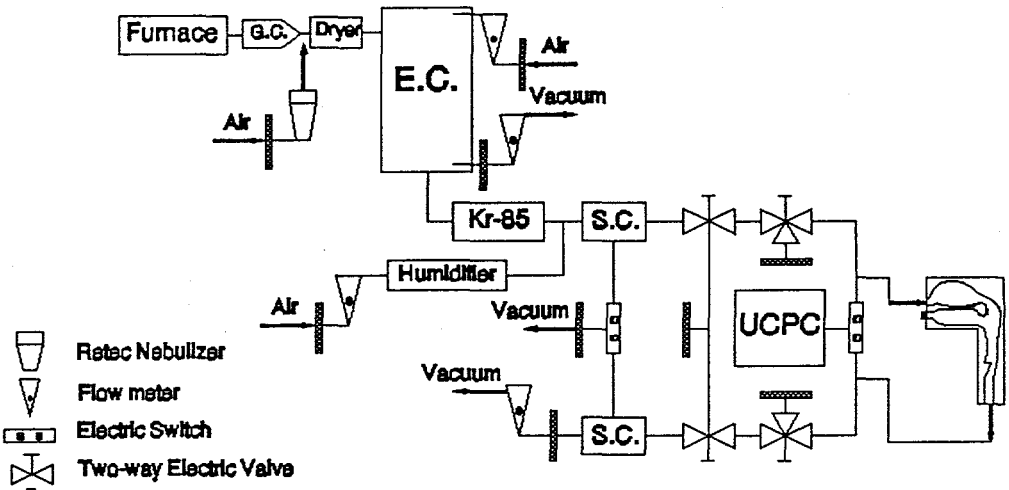

Retec Nebulizer
Flow meter
Electric Switch
Two-way Electric Valve
Three-way Electric Valve
Filter

UCPC: TSI 3025 Particle Counter
E. C.: TSI 3071 Electrostatic Classifier
S. C.: Sampling Chamber
G. C.: Glass Chamber

Calculation of Total Deposition Fraction of Ultrafine Aerosols in Human Extrathoracic and Thoracic Regions

Kuo-Hsi Cheng and David L. Swift

Division of Environmental Health Engineering
The Johns Hopkins University
School of Hygiene and Public Health
615 N. Wolfe St. Baltimore, MD 21205

ABSTRACT

Total deposition fraction during inspiration and expiration can be considered as an index of cumulative doses of inhaled particles. We have calculated the total deposition fraction of ultrafine aerosols from 5 to 200 nm in the extrathoracic airways and in the lung for two breathing rates, 7.5 and 15 $lmin^{-1}$, based on the experimental data of total respiratory deposition measured by Schiller et al. (1988) and the empirical equations of extrathoracic airways developed by Cheng et al. (1993) and Swift et al. (1993). Our results indicated that the contribution of particle deposition during expiration to the total deposition fraction in the nasal and oral passages was important for particle size less than 20 nm. The total lung deposition fraction increased as particle size increased from 5 to 20 nm, and decreased consistently thereafter until particle diameter reached 200 nm. These trends were observed for both nasal and oral breathing regardless of respiratory flow rate.

INTRODUCTION:

Inhalation is the major route of entry for airborne contaminants that include gases, vapors, and particulate matters. Many environmental aerosols which can produce tissue damage and toxic effects in the respiratory tract are in the size range of ultrafine particles from 1 to 200 nm. Radon progeny that have been linked to excess cases of lung cancer in underground miners are ultrafine particles whose sizes are mostly smaller than 200 nm in the indoor environment. Environmental tobacco smoke (ETS), one of the major potential sources of indoor pollutants, also contains a substantial number of nanometer particles. Thus, information regarding deposition of ultrafine particles in the respiratory airway is essential to an understanding of inhalation toxicology and dosimetry of inhaled particles.

The respiratory tract can be conveniently described as two distinct regions: (1) the extrathoracic region, consisting of the nasal and oral airways; and, (2) the thoracic region, including trachea, bronchi, and alveoli. Because of the conditioning

function that warms and humidifies the inspired air, the upper airways are susceptible to infections and respiratory diseases. Particle deposition in the extrathoracic region not only is considered as the first defense of the lung against particles penetrating into the more distal airways, but has increasing concern in the toxicity of deposited particles in this region per se. The development of dosimetric models has been historically focused on the tracheobronchial (TB) region at which the majority of lung cancer were found. For assessing potential human health risks and for understanding the basic toxicological issues, there is a growing interest in developing dosimetric models for different anatomical regions of the respiratory tract.

We have calculated the total deposition fraction of ultrafine particles from 5 to 200 nm in the extrathoracic airways and in the lung for two respiratory flow rates (7.5 and 15 $lmin^{-1}$) based on the experimental data of total respiratory deposition by Schiller et al. (1988) and the empirical equations developed by Cheng et al. (1993) and Swift et al.(1993). Martonen and Yang (1993) have done a simulation of the total deposition fraction of ultrafine particles from 4.9 to 98 nm in the extrathoracic and thoracic regions for the laboratory rat. This study will provide a comparison of particle deposition in the respiratory tract between the human and laboratory animals which are usually used as surrogates for research in inhalation toxicology.

It is important to make a clear distinction between deposition efficiency and deposition fraction. Deposition efficiency is defined as the percentage of particles traversing the previous region the deposit in a specific region, while deposition fraction is the percentage that is removed from the total inhaled particles by a specific region. In this study, we defined the total deposition fraction in a region of interest as the cumulative deposition of particles for both inhalation and exhalation during an entire respiratory cycle.

METHODS:

The entire respiratory tract can be considered as a system of many filters connected in series for particle deposition. For an entire cycle of nasal breathing, three different filters are involved: (1) the nose, nasopharynx, and larynx during inspiration (denoted N_{in}), (2) the lung during both inspiration and expiration (denoted L), and (3) the larynx, nasopharynx, and nose during expiration (denoted N_{out}). The deposition efficiency of ultrafine particles in these three regions is denoted as ε_{Nin}, $\varepsilon_{L,1}$, and ε_{Nout}, respectively. Thus, the total respiratory deposition efficiency for nasal breathing (ε_N) can be mathematically formulated as

$$\varepsilon_N = \varepsilon_{Nin} + (1 - \varepsilon_{Nin})\ \varepsilon_{L,1} + (1 - \varepsilon_{Nin})\ (1 - \varepsilon_{L,1})\ \varepsilon_{Nout} \qquad (1)$$

Similar relationship is employed to establish the equation of particle deposition for oral breathing. The total respiratory

deposition efficiency for oral breathing (ε_M) is given by

$$\varepsilon_M = \varepsilon_{Min} + (1 - \varepsilon_{Min})\ \varepsilon_{L,2} + (1 - \varepsilon_{Min})\ (1 - \varepsilon_{L,2})\ \varepsilon_{Mout} \quad (2)$$

where ε_{Min}, $\varepsilon_{L,2}$, and ε_{Mout} is the deposition efficiency for the oral airway during inspiration, the lung during inspiration and expiration, and the oral airway during expiration, respectively.

The data of total respiratory deposition efficiency for the nasal and oral breathing, ε_N and ε_M, used in this study were taken from Schiller et al. (1988) using monodisperse silver aerosols. They determined the total deposition of ultrafine particles by measuring the mean particle number concentration in inspired and expired air of 4 human subjects for a variety of breathing patterns. The inspiratory and expiratory nasal deposition efficiency was calculated from the following equations (Swift et al., 1993):

$$\varepsilon_{Nin} = 1 - \exp(-12.66\ D^{1/2}\ Q^{-1/8}) \quad (3)$$

$$\varepsilon_{Nout} = 1 - \exp(-15.0\ D^{1/2}\ Q^{-1/8}) \quad (4)$$

where D is the diffusion coefficient in cm^2sec^{-1} and Q is the flow rate in $lmin^{-1}$. The inspiratory and expiratory oral deposition efficiency was obtained from (Cheng et al., 1993)

$$\varepsilon_{Min} = 1 - \exp(-9.925\ D^{1/2}\ Q^{-1/8}) \quad (5)$$

$$\varepsilon_{Mout} = 1 - \exp(-8.51\ D^{1/2}\ Q^{-1/8}) \quad (6)$$

in which D and Q are defined as above. Swift et al. (1993) and Cheng et al. (1993) developed these empirical equations based on a series of experimental measurements of aerosol deposition in replicate models which were constructed from post mortem casts and magnetic resonance (MR) images.

Given the data of total respiratory deposition and deposition efficiency in the nasal and oral airways, $\varepsilon_{L,1}$ and $\varepsilon_{L,2}$ in equations (1) and (2) can be calculated. The total lung deposition fraction relative to the initial aerosol entering the nostrils is thus equal to $(1 - \varepsilon_{Nin})\varepsilon_{L,1}$ for nasal breathing and $(1 - \varepsilon_{Min})\varepsilon_{L,2}$ for oral breathing. The total nasal deposition fraction for an entire breathing cycle is the sum of particle deposition during inhalation and exhalation, which equals $\varepsilon_{Ni} + (1 - \varepsilon_{Nin})(1 - \varepsilon_{L,1})\varepsilon_{Nout}$. For oral breathing, the total oral deposition fraction is equal to $\varepsilon_{Mi} + (1 - \varepsilon_{Min})(1 - \varepsilon_{L,2})\varepsilon_{Mout}$.

RESULTS:

Our results indicated that the contribution of particle deposition during expiration to the total deposition fraction in the nasal and oral airways was important for particle size less than 20 nm. The total lung deposition fraction increased as particle size increased from 5 to 20 nm, and decreased consistently thereafter until particle diameter reached 200 nm. It is interesting to note that these trends were observed for both nasal and oral breathing regardless of respiratory flow rate.

Tables 1 and 2 summarize the total deposition fraction of ultrafine particles in the nasal airway and in the lung for two flow rates. The effect of increase of flow rate was to decrease the total nasal deposition fraction and to increase the total lung deposition fraction for any given particle size. For flow rate equal to 7.5 $lmin^{-1}$, the total nasal deposition fraction reached approximately 57% for 5 nm particles and decreased to only 3% for 200 nm particles. The contribution of nasal deposition during expiration was very significant for 5 nm particles; there was an increase of 20% deposition fraction during expiration in addition to the inspiratory deposition efficiency, 37%. The total lung deposition fraction was about 15% at 5 nm, reached 35% at 20 nm, and decreased down to 10% at 200 nm.

For flow rate equal to 15 $lmin^{-1}$, the total nasal deposition fraction was 44% for 5 nm particles and 3% for 200 nm particles. The enhancement of nasal deposition fraction during expiration was 10% for 5 nm particles and only 1 to 3% for particles larger than 50 nm. The total lung deposition fraction was about 41% at 5 nm, rose up to 50% at 20 nm, and dropped down to 12% at 200 nm.

Tables 3 and 4 show the total deposition fraction of ultrafine particles in the oral airway and in the lung for two flow rates. Like the effect of flow rate on particle deposition for nasal breathing, elevated level of breathing rate tended to decrease the total oral deposition fraction and to increase the total lung deposition fraction for given particle size. For oral breathing of 7.5 $lmin^{-1}$, the total oral deposition fraction was about 42% for 5 nm particles and less than 5% for particles larger than 50 nm. The enhancement of oral deposition fraction during expiration, 12%, was not as significant as that of nasal expiratory deposition for 5 nm particles. The total lung deposition fraction was 25% at 5 nm, increased to 40% at 20 nm, and decreased to 11% at 200 nm.

For oral breathing of 15 $lmin^{-1}$, the total oral deposition fraction was 34% for 5 nm particles and 2% for 200 nm particles. The enhancement of oral deposition fraction during expiration at this flow rate was only 6% for 5 nm particles. The total lung deposition fraction was 46% at 5 nm, increased to 54% at 20 nm, and decreased to 13% at 200 nm.

Figures 1 and 2 show the composite results of total deposition fraction in the extrathoracic and thoracic regions for two breathing patterns and two flow rates. The curves were best fitted by the Spline function between data points.

DISCUSSION:

Deposition of ultrafine aerosols in the nasal and oral airways has been studies by Cheng et al. (1993) and Swift et al. (1993) using human replicate physical casts. They have developed empirical equations of deposition efficiency of ultrafine particles

in the nasal and oral passages for both inhalation and exhalation, as discussed above. However, there is no information with respect to total removal fraction of inhaled aerosols in the extrathoracic airways for an entire breathing cycle. Fractional losses relative to inhaled aerosols in the nose and mouth during inhalation and exhalation can be considered as an index of cumulative doses to the extrathoracic airways.

Due to difficulties of experimental methodology in measuring lung deposition, only inspiratory deposition efficiency relative to aerosols entering larynx has been experimentally determined by Cohen et al. (1990) in a human TB cast for the first seven airway generations. Most of the deposition data of ultrafine particles in the TB region were obtained from theoretical predictions that assumed laminar air flow in a simple cylindrical tube with the diameter equivalent to the corresponding airway. Since assumption about particle deposition in the extrathoracic airways was required to perform this mathematical modeling, the validity of theoretical prediction of lung deposition might be questioned when more experimental studies came along. Thus, it is necessary to estimate the total lung deposition fraction based on recent experimental measurements obtained from human subjects and replicate casts.

The results of this study showed that there was a substantial fraction of inhaled particles less than 10 nm deposited in the nasal and oral airways. A significant fraction of total deposition in the extrathoracic region was contributed by the process of expiration. This implies that inspiratory deposition efficiency may not be adequate for assessing the dose to the upper airways associated with exposure to unattached radon progeny. The total deposition fraction of inhaled particles is a more appropriate definition of cumulative dose, from which a better dose-response relationship can be established for health risk analysis.

It should be noted that the highest total deposition fraction in the lung occurred for particles of diameter of 20 nm, regardless of breathing pattern and flow rate. An increase of flow rate from 7.5 to 15 $lmin^{-1}$ was found to significantly increase the total deposition fraction in the lung. The reasons for these findings are not clear and need further research in investigating the mechanism of deposition of ultrafine particles in the conducting airways and alveolar region. There is also a need to study total deposition fraction in the respiratory tract for particles less than 5 nm whose sizes correspond to unattached radon progeny.

REFERENCES:

Cheng, Y-S, Su, Y-F, Yeh, H-C, Swift, D. L. Deposition of Thoron Progeny in Human Head Airways. Aerosol Sci. & Tech., 18, 359 - 375 (1993)

Martonen, T. B. and Yang Y. Simulation of Aerosol Deposition in Extrathoracic and Laryngeal Passages of the Laboratory Rat. J. of Aerosol Sci. Vol 24, No 1, 103 - 114 (1993).

Schiller, Ch. F., Gebhart J., Heyder, J., Rudolf, G., and Stahlhofen, W. Deposition of Monodisperse Insoluble Aerosol Particles in the 0.005 and 0.2 μm Size Range within the Human Respiratory Tract. Ann. Occup. Hyg. Vol 32, 41 - 49 Supplement 1 (1988)

Swift, D. L., Cheng, Y-S, Su, Y-F, and Yeh, H-C Ultrafine Aerosol Deposition in the Human Nasal and Oral Passages Inhaled Particles VII, National Radiological Protection Board, UK (1993)

Table 1 Human Deposition Data of Ultrafine Particles in the Nose and in the Lung for Nasal Breathing at Flow Rate Equal to 7.5 lpm

Particle Size (nm)	Total Respiratory Deposition Efficiency[1]	Nasal Deposition Efficiency[2]		Overall Lung Deposition Efficiency	Cumulative Nasal Deposition Fraction	Cumulative Lung Deposition Fraction
		Inspiration	Expiration			
5	0.72	0.37	0.42	0.24	0.57	0.15
10	0.62	0.20	0.24	0.38	0.32	0.30
20	0.53	0.11	0.13	0.39	0.18	0.35
30	0.45	0.07	0.09	0.35	0.13	0.32
40	0.39	0.06	0.07	0.31	0.10	0.29
50	0.34	0.05	0.06	0.27	0.09	0.25
60	0.30	0.04	0.05	0.24	0.07	0.23
70	0.28	0.04	0.04	0.22	0.07	0.21
80	0.25	0.03	0.04	0.20	0.06	0.19
90	0.23	0.03	0.03	0.18	0.05	0.18
100	0.21	0.03	0.03	0.16	0.05	0.16
150	0.15	0.02	0.02	0.11	0.04	0.11
200	0.13	0.01	0.02	0.10	0.03	0.10

* 1. Total respiratory deposition data were taken from Schiller et al. (1988)
2. Nasal deposition data were calculated from the empirical equations developed by Cheng et al. (1993) and Swift et al. (1993)

Table 2 Human Deposition Data of Ultrafine Particles in the Nose and in the Lung for Nasal Breathing at Flow Rate Equal to 15 lpm

Particle Size (nm)	Total Respiratory Deposition Efficiency[1]	Nasal Deposition Efficiency[2]		Overall Lung Deposition Efficiency	Cumulative Nasal Deposition Fraction	Cumulative Lung Deposition Fraction
		Inspiration	Expiration			
5	0.85	0.34	0.39	0.63	0.44	0.41
10	0.72	0.19	0.22	0.56	0.27	0.45
20	0.65	0.10	0.12	0.56	0.15	0.50
30	0.56	0.07	0.08	0.49	0.11	0.45
40	0.50	0.05	0.06	0.44	0.09	0.41
50	0.44	0.04	0.05	0.38	0.07	0.37
60	0.39	0.04	0.04	0.34	0.06	0.33
70	0.35	0.03	0.04	0.30	0.06	0.29
80	0.32	0.03	0.03	0.28	0.05	0.27
90	0.29	0.03	0.03	0.25	0.05	0.24
100	0.27	0.02	0.03	0.23	0.04	0.23
150	0.20	0.02	0.02	0.17	0.03	0.17
200	0.15	0.01	0.02	0.12	0.03	0.12

* 1. Total respiratory deposition data were taken from Schiller et al. (1988)
2. Nasal deposition data were calculated from the empirical equations developed by Cheng et al. (1993) and Swift et al. (1993)

Table 3 Human Deposition Data of Ultrafine Particles in the Mouth and in the Lung for Oral Breathing at Flow Rate Equal to 7.5 lpm

Particle Size (nm)	Total Respiratory Deposition Efficiency[1]	Oral Deposition Efficiency[2]		Overall Lung Deposition Efficiency	Cumulative Oral Deposition Fraction	Cumulative Lung Deposition Fraction
		Inspiration	Expiration			
5	0.67	0.30	0.26	0.36	0.42	0.25
10	0.62	0.16	0.14	0.47	0.23	0.39
20	0.53	0.09	0.08	0.44	0.13	0.40
30	0.45	0.06	0.05	0.38	0.09	0.36
40	0.39	0.05	0.04	0.34	0.07	0.32
50	0.34	0.04	0.03	0.29	0.06	0.28
60	0.30	0.03	0.03	0.26	0.05	0.25
70	0.28	0.03	0.02	0.24	0.05	0.23
80	0.25	0.02	0.02	0.22	0.04	0.21
90	0.23	0.02	0.02	0.20	0.04	0.19
100	0.21	0.02	0.02	0.18	0.03	0.18
150	0.15	0.02	0.01	0.13	0.03	0.12
200	0.13	0.01	0.01	0.11	0.02	0.11

* 1. Total respiratory deposition data were taken from Schiller et al. (1988)
2. Oral deposition data were calculated from the empirical equations developed by Cheng et al. (1993) and Swift et al (1993)

Table 4 Human Deposition Data of Ultrafine Particles in the Mouth and in the Lung for Oral Breathing at Flow Rate Equal to 15 lpm

Particle Size (nm)	Total Respiratory Deposition Efficiency[1]	Oral Deposition Efficiency[2]		Overall Lung Deposition Efficiency	Cumulative Oral Deposition Fraction	Cumulative Lung Deposition Fraction
		Inspiration	Expiration			
5	0.80	0.28	0.25	0.63	0.34	0.46
10	0.72	0.15	0.13	0.62	0.19	0.53
20	0.65	0.08	0.07	0.59	0.11	0.54
30	0.56	0.05	0.05	0.51	0.08	0.48
40	0.50	0.04	0.04	0.46	0.06	0.44
50	0.44	0.03	0.03	0.40	0.05	0.39
60	0.39	0.03	0.02	0.36	0.04	0.35
70	0.35	0.03	0.02	0.32	0.04	0.31
80	0.32	0.02	0.02	0.29	0.04	0.28
90	0.29	0.02	0.02	0.26	0.03	0.26
100	0.27	0.02	0.02	0.24	0.03	0.24
150	0.20	0.01	0.01	0.18	0.02	0.18
200	0.15	0.01	0.01	0.13	0.02	0.13

* 1. Total respiratory deposition data were taken from Schiller et al. (1988)
2. Oral deposition data were calculated from the empirical equations developed by Cheng et al. (1993) and Swift et al (1993)

Figure 1 Total Deposition Fraction of Ultrafine Particles in the Thoracic Region

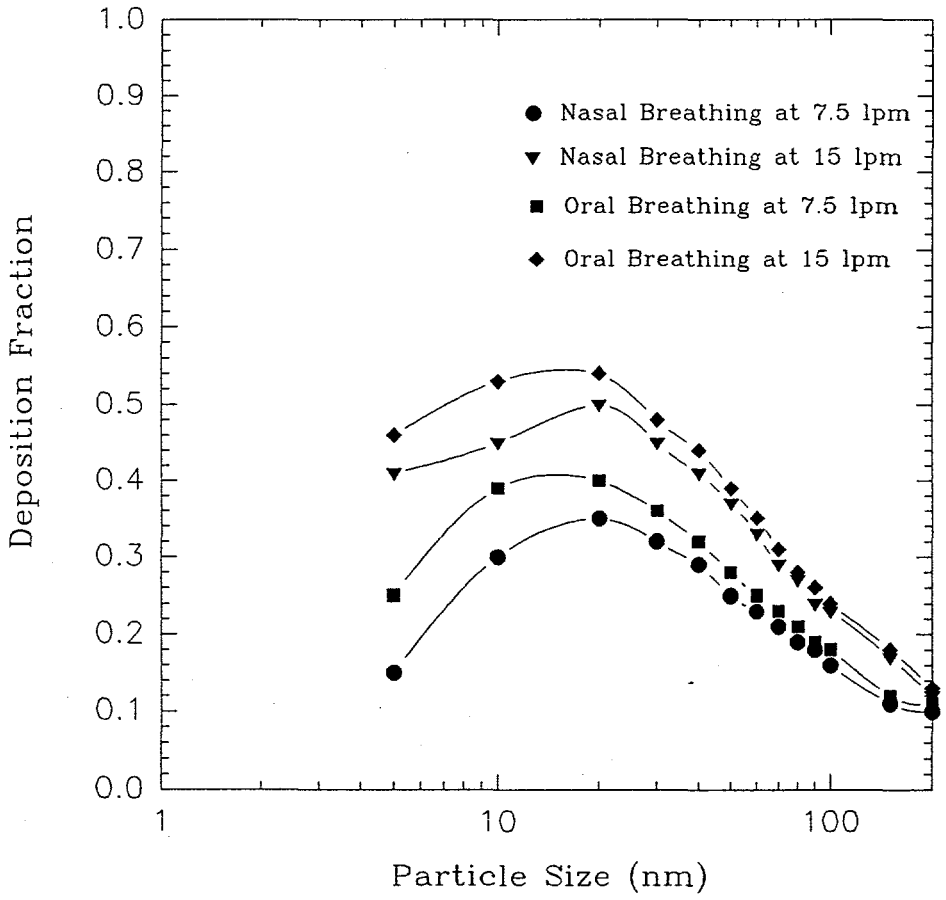

Figure 2 Total Deposition Fraction of Ultrafine Particles in the Extrathoracic Region